Molecular Phylogenetics and Evolution 187 (2023) 107872

Contents lists available at ScienceDirect

Molecular Phylogenetics and Evolution

journal homepage: www.elsevier.com/locate/ympev

Updated phylogeny of Vestimentifera (Siboglinidae, Polychaeta, Annelida) based on mitochondrial genomes, with a new species

Marina F. McCowin [a,*], Patrick C. Collins [b], Greg W. Rouse [a,c,*]

[a] Scripps Institution of Oceanography, University of California San Diego, La Jolla, CA 92093-0202, USA
[b] Queen's University Belfast, Belfast, Co. Antrim, BT9 5DL, Northern Ireland
[c] South Australian Museum, North Terrace, Adelaide, SA 5000, Australia

ARTICLE INFO

Keywords:
Vestimentifera
Siboglinidae
Tubeworms
Chemosynthetic
Mitochondrial genome
New species
Deep-sea taxonomy

ABSTRACT

Siboglinid tubeworms are found at chemosynthetic environments worldwide and the Vestimentifera clade is particularly well known for their reliance on chemoautotrophic bacterial symbionts for nutrition. The mitochondrial genomes have been published for nine vestimentiferan species to date. This study provides new complete mitochondrial genomes for ten further Vestimentifera, including the first mitochondrial genomes sequenced for *Alaysia spiralis*, *Arcovestia ivanovi*, *Lamellibrachia barhami*, *Lamellibrachia columna*, *Lamellibrachia donwalshi*, and unnamed species of *Alaysia* and *Oasisia*. Phylogenetic analyses combining fifteen mitochondrial genes and the nuclear 18S rRNA gene recovered *Lamellibrachia* as sister to the remaining Vestimentifera and *Riftia pachyptila* as separate from the other vent-endemic taxa. Implications and auxiliary analyses regarding differing phylogenetic tree topologies, substitution saturation, ancestral state reconstruction, and divergence estimates are also discussed. Additionally, a new species of *Alaysia* is described from the Manus Basin.

1. Introduction

Tubeworms of the rank-free clade Vestimentifera within Siboglinidae (Annelida, Polychaeta, Siboglinidae) are found at deep-sea chemosynthetic environments such as hydrothermal vents, seeps, and organic falls (Bright and Lallier, 2010; Feldman et al., 1998; Jones, 1981; Webb, 1969). Vestimentifera, erected by Jones (1985) and later revised as an informal lineage within Siboglinidae Caullery, 1914 (Hilário et al., 2011; Pleijel et al., 2009; Rouse and Fauchald, 1997), encompasses ten currently accepted genera that are known for their reliance on symbioses with chemoautotrophic bacteria. These bacteria metabolize hydrogen sulfide, providing nutrition for the host worms, which lack a mouth and gut as adults and rely on the organic compounds provided by their endosymbionts (Bright and Lallier, 2010). Six genera are endemic to hydrothermal vents in the Pacific: *Riftia* Jones, 1981, *Ridgeia* Jones, 1985, *Tevnia* Jones, 1985, *Oasisia* Jones, 1985, *Alaysia* Southward, 1991, and *Arcovestia* Southward and Galkin, 1997 with no vent-only taxa known from other oceans.

Alaysia spiralis Southward, 1991 was originally described from the Lau Back-Arc basin (near Tonga) and *Arcovestia ivanovi* Southward and Galkin, 1997 from the Manus Basin (Papua New Guinea). The two are differentiated by their outer sheath lamellae (present in *Alaysia*, absent in *Arcovestia*) and obturaculum characteristics (Southward and Galkin, 1997). Photos of specimens of each species (including *Alaysia spiralis* from near the type locality) are presented in Fig. 1. Both of these vestimentiferan species grow in low density patches at the Manus Basin vents around areas of diffuse flow and provide crucial habitat for many other organisms that contribute to the biodiversity in the basin (Samadi et al., 2015). This area has been a focus of study in recent years (Kojima et al., 2002; Samadi et al., 2015; Van Audenhaege et al., 2019; Watanabe and Kojima, 2015) because areas have been slated for deep-sea mining, which would likely have deleterious effects on the biodiversity, connectivity, and community structure of the these areas (Levin et al., 2016; Miller et al., 2018). Mining could be especially damaging to taxa endemic to the site or region, and may have additional harmful effects that extend beyond the mining site (impacts from sediment plumes, noise and light pollution, etc), though there is a current moratorium on mining in the region (Levin et al., 2016). Sampling has been conducted in an attempt to catalog the existing biodiversity to inform management practices (Collins et al., 2012; Kojima et al., 2002; Samadi et al., 2015; Van Audenhaege et al., 2019). This sampling has revealed multiple species of Vestimentifera, including *Lamellibrachia* Webb, 1969, *Arcovestia*, *Alaysia*, and *Paraescarpia* Southward et al., 2002 (Samadi et al., 2015; Van Audenhaege et al., 2019), and some putative new species of

* Correspondiing author.
E-mail addresses: marruda@ucsd.edu (M.F. McCowin), grouse@ucsd.edu (G.W. Rouse).

https://doi.org/10.1016/j.ympev.2023.107872
Received 24 March 2023; Received in revised form 22 June 2023; Accepted 6 July 2023
Available online 13 July 2023

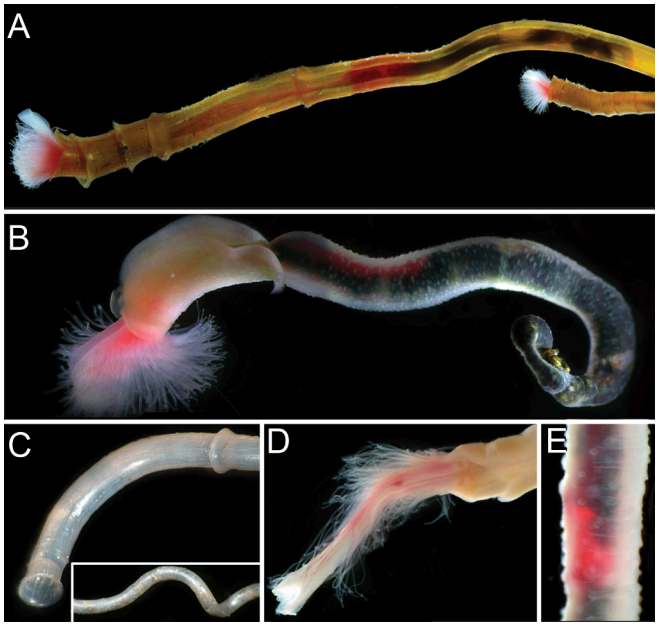

Fig. 1. Photographs of *Arcovestia ivanovi* and *Alaysia spiralis*. (A) *Arcovestia ivanovi* (GenBank accession number FJ667530) anterior in tube. (B) *Arcovestia ivanovi* (same specimen) whole, dissected out of tube. (C) *Alaysia spiralis* (GenBank accession number FJ667536) tube anterior showing flanges and spiraling (inset). (D) *Alaysia spiralis* (GenBank accession number FJ667536) anterior, removed from tube. (E) *Alaysia spiralis* trunk detail, showing papillae.

Alaysia in this region (Kojima et al., 2003, unpublished data). Many questions remain unanswered about *Alaysia* and *Arcovestia*, including their placement in the overall phylogeny of Vestimentifera, which has not yet been established with ample molecular data. There have only been two phylogenetic studies with molecular data for *Alaysia* or *Arcovestia* to date (Kojima et al., 2003, 2002). While Kojima et al. (2002) provided identification of *Arcovestia ivanovi* sequences based on their proximity to the type locality, only tentative identifications of potential *Alaysia* species could be reported by Kojima et al. (2003) due to a lack of *A. spiralis* material from the type locality in the Lau Back-Arc Basin. Neither study confidently placed *Alaysia* or *Arcovestia* in the vestimentiferan phylogeny owing to limited taxonomic sampling and the use of mitochondrial COI data only.

Previous phylogenetic analyses of Vestimentifera have utilized morphological characters, Sanger-sequenced mitochondrial and nuclear fragments, microsatellites, and (in recent years) whole mitochondrial genomes to describe new species and elucidate relationships between species. However, statistical support for many relationships within Vestimentifera have remained generally low for studies with small numbers of markers (Halanych, 2005) and nuclear data is often either limited to a few species or uninformative (Halanych et al., 2001). In recent years, the mitochondrial genomes of sixteen members of Siboglinidae have already proven valuable in resolving the siboglinid phylogeny (Li et al., 2015; Patra et al., 2016; Sun et al., 2018). However, the mitochondrial genomes of *Alaysia* and *Arcovestia* were missing from these datasets. This study adds the mitochondrial genomes for *Alaysia spiralis* and *Arcovestia ivanovi*, as well as eight other members of Vestimentifera, including a new species of *Alaysia*, a new species of *Oasisia*, multiple *Lamellibrachia* species, and additional samples of *Riftia pachyptila* and *Escarpia spicata* Jones, 1985. Nucleotide and amino-acid-translated phylogenies are generated from the newly sequenced mitochondrial genome data (13 protein coding genes and 2 ribosomal RNA genes) and nuclear 18S gene. Genetic data from this study reveals two putatively new species of *Alaysia* and includes a formal description for one of them.

2. Methods

2.1. Sampling and morphological analyses

Vestimentifera samples were collected and subsampled for DNA on various dives between 1990 and 2018. Fig. 2 shows sampling and type localities for *Alaysia* and *Arcovestia*. Twelve *Alaysia spiralis* specimens were borrowed from the South Australian Museum (SAM) for analysis, originally collected from the "Snowcap" and "Satanic Mills" sites in the Manus Basin in 2000. One *Alaysia spiralis* specimen was also collected by the ROV *Jason II* at a vent near the species type locality in the Lau Back-Arc Basin, at 1,905 m in 2005. While the voucher material for this specimen was lost/destroyed, photographs and sequences associated with the specimen have been made available (see Fig. 1 and Table 2). Two *Arcovestia ivanovi* specimens were collected by the ROV *Jason II* at a vent at approximately 2,200 m in the Lau Back-Arc Basin in 2005. Four *A. ivanovi* specimens were borrowed from SAM, originally sampled from the "Snowcap" and "Satanic Mills" sites in the Manus Basin in 2000 (CSIRO Binatang 2000 Expedition). Eleven specimens of the new species of *Alaysia* described here (*Alaysia solwarawarriors* sp. nov.) were also collected from the "South Su" site in the Manus Basin in 2007, and three specimens of a different putative new species of *Alaysia* (*Alaysia* sp. nov. 1) were collected from the "Snowcap" and "Satanic Mills" sites in the Manus Basin in 2000. Additional sampling details for these specimens and others used in genetic analysis are also listed in Table 1 (samples for which whole mitochondrial genomes were sequenced) and Table 2 (all samples used in various phylogenetic analyses). The map of Manus and Lau Basin sampling localities (Fig. 2) was created in RStudio using R v.4.1.3 with the package marmap v.1.0.6 (Pante and Simon-Bouhet, 2013).

For molecular analyses, whole or partially whole animals were either frozen and kept at −80 °C or preserved in 95% ethanol in their chitinous tubes. The *Alaysia solwarawarriors* sp. nov. holotype was fixed and stored in 95% ethanol, and later the anterior was dissected out from the tube to facilitate photography and measurements. Specimen tissues adhered to their semi-transparent chitinous tube walls during fixing and preservation, so photographs and measurements were taken through the semi-transparent tubes when possible, to keep the specimen intact. The specimen was photographed using a Canon T7i camera and Leica MZ12.5 stereo microscope. Measurements were made of the

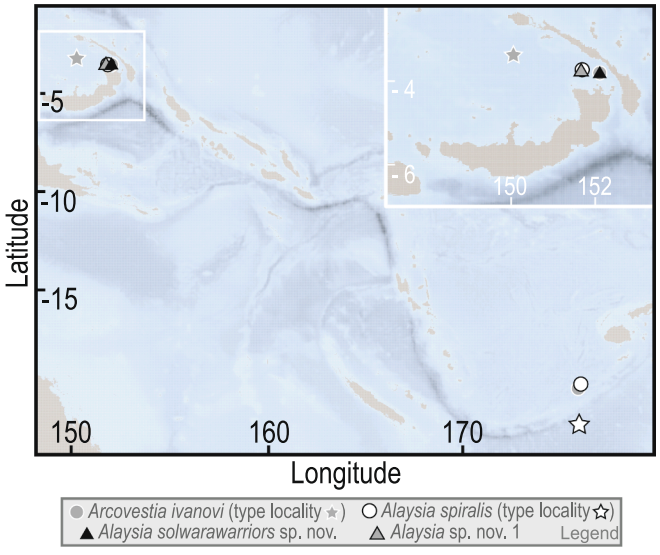

Fig. 2. Map of sampling areas in Manus and Lau Back-Arc basins. Type localities of currently described species represented by stars. Type localities of putative new species represented by triangles. All other sampling localities represented by circles.

Table 1
Sequencing information and origin of sequenced terminals, vouchers, and GenBank accession numbers for whole mitochondrial genome data. Newly sequenced mitochondrial genomes are set in bold. An asterisk () indicates this study reported that all genes were encoded on the same strand, but did not explicitly state which strand; however, reported AT-richness suggests genes are likely encoded on the positive strand. Abbreviations: SIO-BIC, Scripps Institution of Oceanography Benthic Invertebrate Collection; SAM, South Australian Museum.

Scientific Name	Locality	Depth	Latitude	Longitude	Habitat	Total Length	Coding Strand	Average Sequencing Coverage	AT Content	GC Content	GenBank Accession Number	Voucher or Reference
Alaysia* sp. nov. *2	**South Su, Manus Basin, Bismarck Sea**	**1452**	**−3.811**	**152.103**	**vent**	**14,981**	**+**	**234**	**65.20%**	**34.80%**	**ON929999**	**SIO-BIC A12497**
Alaysia spiralis	**Eastern Manus Basin, Bismarck Sea**	**1645–1735**	**−3.728**	**151.669**	**vent**	**15,040**	**–**	**306**	**65.54%**	**34.46%**	**ON929998**	**SAM E8131**
Arcovestia ivanovi	**South Su, Manus Basin, Bismarck Sea**	**1452**	**−3.811**	**152.103**	**vent**	**14,953**	**–**	**199**	**65.75%**	**34.25%**	**ON930000**	**SIO-BIC A12501**
Escarpia "laminata"	Mississippi Canyon, US	~ 754	28.19	−89.8	seep	15,445	+*	232	66.09%	33.91%	KJ789161	Li et al. 2015
Escarpia spicata	**West Florida Escarpment, Gulf of Mexico**	**3314**	**26.04**	**−84.91**	**seep**	**15,150**	**–**	**147**	**63.78%**	**36.22%**	**ON929994**	**SIO-BIC A12974**
Escarpia spicata	**Jaco Scar, Costa Rica Margin**	**1798–1908**	**9.12**	**−84.84**	**seep**	**15,168**	**+**	**151**	**63.75%**	**36.25%**	**ON929996**	**SIO-BIC A8327**
Lamellibrachia barhami	**Mound Jaguar, Costa Rica Margin**	**1909**	**9.66**	**−85.88**	**seep**	**15,019**	**+**	**217**	**65.03%**	**34.97%**	**ON929997**	**SIO-BIC A10173B**
Lamellibrachia columna	**Builder's Pencil, Hikurangi Margin, New Zealand**	**810–817**	**−39.54**	**178.33**	**seep**	**15,115**	**–**	**225**	**63.50%**	**36.50%**	**ON929995**	**SIO-BIC A9468**
Lamellibrachia donwalshi	**Mound 12, Costa Rica Margin**	**990–999**	**8.93**	**−84.31**	**seep**	**14,982**	**+**	**273**	**63.88%**	**35.12%**	**ON929991**	**SIO-BIC A8272**
Lamellibrachia luymesi	Mississippi Canyon, US	~ 754	28.19	−89.8	seep	14,991	+*	67	64.56%	35.44%	KJ89163	Li et al. 2015
Lamellibrachia satsuma	Kagoshima Bay, Japan	110	31.66	130.8	seep	15,037	+	–	65.60%	34.40%	KP987801	Patra et al. 2016
Oasisia alvinae	East Pacific Rise	~ 2630	9.8	−103.94	vent	14,849	+*	39	64.92%	35.08%	KJ789164	Li et al. 2015
Paraescarpia echinospica	Haima cold seep, soouth China Sea	1370–1390	~ 17	~ 110	seep	15,280	*not reported*	–	64.32%	35.68%	MG462707	Sun et al. 2018
Ridgeia piscesae	Southern Explorer Ridge, northeastern Pacific	–	49.76	−130.26	vent	15,002	–	–	57.00%	43.00%	KJ872501	Jun et al. 2016
Riftia pachyptila	East Pacific Rise	~ 2522	9.85	−104.29	vent	14,987	+*	71	66.76	33.24%	KJ789166	Li et al. 2015
Riftia pachyptila	**Matterhorn area, Auka Vent Field, Pescadero Basin, Gulf of California**	**3653.5**	**23.95**	**108.86**	**vent**	**16,566**	**–**	**145**	**65.51%**	**34.49%**	**ON929992**	**SIO-BIC A9493**
Seepiophila jonesi	Mississippi Canyon, US	~ 754	28.19	−89.8	seep	15,092	+*	220	64.83	35.17%	KJ789168	Li et al. 2015
Tevnia jerichonana	East Pacific Rise	~ 2537	9.79	−104.27	vent	14,891	+*	22	64.51%	35.49%	KJ789172	Li et al. 2015
***Oasisia* sp. nov.**	**Southern East Pacific Rise (32S)**	**2338**	**−31.87**	**−112.04**	**vent**	**15,356**	**+**	**161**	**64.80%**	**35.20%**	**ON929993**	**SIO-BIC A11662**
Sclerolinum brattstromi	Storfjorden Fjord, Norway	~ 660	62.45	5.09	–	15,383	+*	23	64.9	35.10%	KJ789167	Li et al. 2015

Table 2
Origin of sequenced terminals, vouchers, and GenBank accession numbers for all phylogenetic analyses, including 16-gene and 3-gene phylogenies and ancestral state reconstruction. Abbreviations: SIO-BIC, Scripps Institution of Oceanography Benthic Invertebrate Collection; SAM, South Australian Museum.

Scientific Name	Locality	Depth	Latitude	Longitude	COI	16S	18S	Voucher or Reference
Alaysia sp. A1	Off Hatsushima, Sagami Bay, Japan	830–1230	34.98	139.22	AB088670	–	–	Kojima et al. 2003
Alaysia sp. A2	Daiyon Yonaguni Knoll, South Okinawa Trough, Japan	1320	24.85	122.7	AB088671	–	–	Kojima et al. 2003
Alaysia sp. A3	PACMANUS site, Manus Basin	1660–1710	−3.73	151.67	AB088672	–	–	Kojima et al. 2003
Alaysia sp. A4	North Iheya Knoll, Mid-Okinawa Trough	1050	27.78	126.9	AB088673	–	–	Kojima et al. 2003
***Alaysia* sp. nov. 1**	**"Snowcap", Eastern Manus Basin**	**1645–1735**	**−3.728**	**151.669**	**OP125606-7**	**–**	**–**	**SIO-BIC A14184-5**
***Alaysia* sp. nov. 1**	**"Satanic Mills", Eastern Manus Basin**	**1691**	**−3.725**	**151.674**	**OP125608**	**–**	**–**	**SIO-BIC A14186**
***Alaysia solwarawarriors* sp. nov.**	**"South Su", Manus Basin**	**1452**	**−3.811**	**152.103**	**OP135973-82**	**OP137205-9**	**–**	**SIO-BIC A14167A-E, A14168, A12500, A12503, A12506, A12508**
***Alaysia solwarawarriors* sp. nov.**	**"South Su", Manus Basin**	**1452**	**−3.811**	**152.103**	**ON929999**	**ON929999**	**OP137200**	**SIO-BIC A12497**
Alaysia spiralis	**Lau Back-arc Basin**	**1905**	**−20.054**	**176.135**	**FJ667536**	**–**	**–**	**this study**
Alaysia spiralis	**"Snowcap", Eastern Manus Basin**	**1645–1735**	**−3.728**	**151.669**	**OP131318-26**	**–**	**–**	**SAM E8119, E8121-6, E8128-9**
Alaysia spiralis	**"Snowcap", Eastern Manus Basin**	**1645–1735**	**−3.728**	**151.669**	**ON929998**	**ON929998**	**OP137198**	**SAM E8131**
Alaysia spiralis	**"Satanic Mills", Eastern Manus Basin**	**1691**	**−3.725**	**151.674**	**OP131729**	**–**		**SAM E3632a**
Arcovestia ivanovi	**Lau Back-arc Basin**	**2719–2721**	**−20.318**	**176.137**	**OP115783-4**	**–**	**–**	**SIO-BIC A14169, A11518**
Arcovestia ivanovi	**Lau Back-arc Basin**	**2719–2721**	**−20.3178**	**176.1373**	**FJ667530**	**–**	**–**	**this study**
Arcovestia ivanovi	**"South Su", Manus Basin**	**1452**	**−3.811**	**152.103**	**OP115786-8**	**–**	**–**	**SIO-BIC A12498, A12510, A12512**
Arcovestia ivanovi	**"South Su", Manus Basin**	**1452**	**−3.811**	**152.103**	**ON930000**	**ON930000**	**OP137199**	**SIO-BIC A12501**
Arcovestia ivanovi	Fenway, PACMANUS site, Manus Basin	1665–1800	−3.728	151.673	MK252699	–	–	Li et al., 2020
Arcovestia ivanovi	PACMANUS site, Manus Basin	1677–1716	0.002	151.673–151.681	MK694787	–	–	Van Audenhaege et al. 2019
Arcovestia ivanovi	PACMANUS or DESMOS site, Manus Basin	1660–1900	−0.03	151.67–151.87	AB073491	–	–	Kojima et al. 2002
Escarpia "laminata"	Mississippi Canyon, US	~ 754	28.19	−89.8	KJ789161	KJ789161	AF168741	Li et al. 2015, Halanych et al., 2001
Escarpia southwardae	Worm Hole seep, West Africa	3189	−4.76	9.94	KC870958	–	–	Cowart et al. 2013
Escarpia spicata	**West Florida Escarpment, Gulf of Mexico**	**3314**	**26.04**	**−84.91**	**ON929994**	**ON929994**	**OP137196**	**SIO-BIC A12974**
Escarpia spicata	**Jaco Scar, Costa Rica Margin**	**1798–1908**	**9.12**	**−84.84**	**ON929996**	**ON929996**	**OP137197**	**SIO-BIC A8327**
Lamellibrachia anaximandri	Nile deep-sea fan, eastern Mediterranean	2129, 1686	32.64, 32.50	29.92, 30.26	EU046616	HM746782	–	Southward et al. 2011
Lamellibrachia barhami	**Mound Jaguar, Costa Rica Margin**	**1909**	**9.66**	**−85.88**	**ON929997**	**ON929997**	**OP137204**	**SIO-BIC A10173B**
Lamellibrachia columna	**Builder's Pencil, Hikurangi Margin, New Zealand**	**810–817**	**−39.54**	**178.33**	**ON929995**	**ON929995**	**OP137202**	**SIO-BIC A9468**
Lamellibrachia donwalshi	**Mound 12, Costa Rica Margin**	**990–999**	**8.93**	**−84.31**	**ON929991**	**ON929991**	**OP137203**	**SIO-BIC A8272**
Lamellibrachia juni	DESMOS site, Manus Basin	1900	−3.7	151.87	AB264603	–	–	Kojima et al. 2006
Lamellibrachia luymesi	Mississippi Canyon, US	~ 754	28.19	−89.8	KJ89163	KJ89163	–	Li et al. 2015
Lamellibrachia satsuma	Kagoshima Bay, Japan	110	31.66	130.8	KP987801	KP987801	FM995543	Patra et al. 2016, Pradillon et al., 2009
Oasisia alvinae	East Pacific Rise	2630	9.8	−103.94	KJ789164	KJ789164	AF168743	Li et al., 2015, Halanych et al., 2001
Oasisia fujikurai	Brother's Caldera, Kermadec Arc	1600	−34.86	179.06	AB242857	–	–	Miura & Kojima 2006
Oasisia sp. nov.	**Southern East Pacific Rise (32S)**	**2338**	**−31.87**	**−112.04**	**ON929993**	**ON929993**	**OP137195**	**SIO-BIC A11662**
Paraescarpia echinospica	Haima cold seep, soouth China Sea	1370–1390	~ 17	~ 110	MG462707	MG462707	–	Sun et al. 2018
Ridgeia piscesae	Southern Explorer Ridge, northeastern Pacific	–	49.76	−130.26	KJ872501	KJ872501	AF168744	Jun et al., 2016, Halanych et al., 2001

(*continued on next page*)

Table 2 (*continued*)

Scientific Name	Locality	Depth	Latitude	Longitude	COI	16S	18S	Voucher or Reference
Riftia pachyptila	**Matterhorn area, Auka Vent Field, Pescadero Basin, Gulf of California**	**3653.5**	**23.95**	**108.86**	**ON929992**	**ON929992**	**OP137201**	**SIO-BIC A9493**
Riftia pachyptila	East Pacific Rise	~ 2522	9.85	−104.29	KJ789166	KJ789166	–	Li et al. 2015
Sclerolinum brattstromi	Storfjorden Fjord, Norway	~ 660	62.45	5.09	KJ789167	KJ789167	AF315061	Li et al. 2015, Halanych et al., 2001
Seepiophila jonesi	Mississippi Canyon, US	~ 754	28.19	−89.8	KJ789168	KJ789168	–	Li et al. 2015
Tevnia jerichonana	East Pacific Rise	2537	9.79	−104.27	KJ789172	KJ789172	AF168746	Li et al., 2015, Halanych et al., 2001

obturaculum, crown, vestimentum, trunk, and tube of the holotype specimen. Type and voucher material is held at the South Australian Museum (SAM), Adelaide, South Australia, Australia and the Scripps Institution of Oceanography Benthic Invertebrate Collection (SIO-BIC), La Jolla, California, USA (accession numbers in Table 1 and Table 2).

2.2. DNA extraction, amplification, and sequencing

DNA was extracted from two *Arcovestia* specimens and seventeen *Alaysia* specimens (various species) with the Zymo Research DNA-Tissue Miniprep kit (Zymo Research, Inc.), following the protocol supplied by the manufacturer. DNA was extracted from the remaining four *Arcovestia* and nine *Alaysia* specimens by the Vrijenhoek lab at the Monterey Bay Aquarium Research Institute (MBARI), Moss Landing, California, USA, before it was donated to SIO-BIC. DNA was also extracted from two *Escarpia spicata* specimens, a single *Oasisia* sp. nov. specimen, a single *Riftia pachyptila* specimen, and a single *Lamellibrachia barhami* Webb, 1969 specimen with the Zymo Research kit and protocol (for later library preparation and mitochondrial genome sequencing, see Table 1). Previous extractions of *Lamellibrachia columna* Southward, 1991 (McCowin et al., 2019), and *Lamellibrachia donwalshi* McCowin & Rouse, 2018 were also utilized for library preparation and mitochondrial genome sequencing (Table 1).

Approximately 500 bp of the mitochondrial gene cytochrome *c* oxidase subunit I (COI) were amplified for each newly-extracted specimen using the vestimentiferan primer *mt*COI primer set COIf and COIr (Nelson and Fisher, 2000) to confirm field identifications of species (see Supplementary Table 1 for primer sequences). For a subset of *Alaysia* and *Arcovestia* samples for which COI did not amplify with these primers, two sets of designed primers targeting shorter regions of the *mt*COI gene (~300 bp and ~ 400 bp) were used (Supplementary Table 1). For the *Alaysia solwarawarriors* sp. nov. holotype, an approximately 400 bp fragment of 16S rRNA (16S) was amplified using the primers 16sArL and 16sbrH (Palumbi, 1996). For one specimen of each *Arcovestia* and *Alaysia* species (excluding *Alaysia* sp. nov. 1) and specimens for which mitochondrial genomes were newly sequenced, approximately 1,770 bp of 18S rRNA were amplified in three fragments using the primer pairs 18S1F and 18S5R, 18Sa2.0 and 18S9R, and 18S3F and 18Sbi (Giribet et al., 1996; Whiting et al., 1997). Amplification was carried out with 12.5 μL of Apex 2.0z RED DNA Polymerase Master Mix (Genesee Scientific), 1 μL each of the appropriate forward and reverse primers (10 μM concentration), 8.5 μL of water, and 2 μL of eluted DNA. Additional PCR reaction details (program parameters for thermal cycler) for each gene can be found in Supplementary Table 1. All PCR products were purified with the ExoSAP-IT protocol (USB, Affymetrix) and sequencing was performed by Eurofins Genomics (Louisville, KY). All sequences were *de novo* assembled in Geneious Prime version 2022.0.2 (Biomatters Ltd.). GenBank accession numbers associated with all Sanger-sequenced individuals can be found in Table 2.

While samples of *Alaysia* sp. nov. 1 were successfully extracted and sequenced, the original voucher material was unfortunately all lost/destroyed. Due to the lack of type material, *Alaysia* sp. nov. 1 cannot be described in this study, but the sequences associated with these specimens have been made available (GenBank accession numbers in Table 2) for future studies.

2.3. Mitochondrial genome Sequencing, Assembly, & annotation

This study used genome skimming (shallow whole genome sequencing followed by bioinformatic separation of mitochondrial reads) to obtain mitochondrial genome data (Trevisan et al., 2019). Prior to library preparation for genome skimming, all extractions were quantified with a Qubit BR Assay kit (ThermoFisher Scientific) following the protocol supplied by the manufacturer. In addition, the quality of all extractions was assessed with gel electrophoresis. Sequencing libraries for a single high-quantity/quality extraction for a representative of *Arcovestia ivanovi*, *Alaysia spiralis*, *Alaysia solwarawarriors* sp. nov., *Lamellibrachia barhami*, *L. columna*, *L. donwalshi*, *Oasisia* sp. nov., and *Riftia pachyptila*, and 2 extractions of *Escarpia spicata* (from different localities) were prepared and sequenced by Novogene (Sacramento, CA, USA) using their Whole Genome Sequencing (WGS) protocol and generating 2 Gb of 150 bp paired-end reads per sample.

Seqkit Version 0.13.2 (Shen et al., 2016) was used to remove duplicates and to assess read numbers and lengths before and after trimming and filtering for quality. Raw reads were trimmed to remove adapter sequences and low quality leading and trailing bases, and filtered with a 4-base sliding window (cutting where average quality per base fell below 15) with Trimmomatic Version 0.39 (Bolger et al., 2014). Reads shorter than 36 bases were removed from the dataset. Trimmed reads were then assembled with Mitofinder Version 1.4 (Allio et al., 2020) with the megahit assembler and tRNA annotation with MiTFi, and the invertebrate mitochondrial DNA genetic code translator (Elzanowski and Ostell, 2019). A reference genomes file for use with MitoFinder was compiled from annelid mitochondrial genomes from GenBank (included only sequences classified as "RefSeq"). Average coverage for each mitochondrial genome (with duplicates removed) ranged between 145x and 306x (Table 1). The resulting annotated contigs were checked with the MITOS web server (Bernt et al., 2013) and annotations were manually checked for inaccuracies. Gene order was identical for all species, with little local length variation, so minor edits were made in Geneious Prime to reconcile any errors. Circularization was not found automatically by MitoFinder, but a circular display of each mitochondrial genome was constructed in Geneious Prime. A putative control region was identified by a noncoding repetitive region in each mitochondrial genome between *trnR* and *trnH* (annotated by MITOS), which is consistent with previously published mitochondrial genomes within Vestimentifera. GenBank accession numbers associated with whole mitochondrial genome sequences can be found in Table 1.

2.4. Phylogenetic analyses using mitochondrial genomes

The thirteen protein-coding genes, 12S rRNA (12S), and 16S rRNA (16S) from the mitochondrial genome assemblies, nuclear 18S rRNA (18S), and data from GenBank (Table 1) were aligned separately with the MAFFT version 7 online server (Katoh et al., 2019) with the direction of nucleotide sequences set to adjust according to the first sequence (extremely slow) and all other settings default (nucleotide dataset). All thirteen mitochondrial protein-coding genes were also translated into

amino acids in Geneious Prime (to be combined with the non-protein-coding 12S, 16S, and 18S nucleotide data to form the amino-acid-translated dataset). Appropriate models for each gene partition (nucleotide and amino-acid-translated separate) were chosen by ModelTest-NG v.0.1.6 under the Akaike Information Criterion (AICc) (Supplementary Table 3). The datasets (nucleotide and amino-acid-translated) were then concatenated. Each of the two resulting datasets contained 13 mitochondrial protein-coding genes (either in nucleotide or amino-acid-translated format), 12S, 16S, and nuclear 18S. Maximum likelihood (ML) analyses were conducted with each of the nucleotide and amino-acid-translated datasets with the RAxML GUI interface v. 2.0.2 (Edler et al., 2020) using RAxML-ng v. 1.0.1 (Kozlov et al., 2019) with each partition assigned the appropriate model from ModelTest-NG (Supplementary Table 3). Additional ML analyses was conducted for the nucleotide dataset with the third codon positions of protein coding genes partitioned separately from the first and second positions, and with each of the codon positions partitioned separately (these partitions were re-tested for appropriate models using ModelTest-NG and IQTree, and a 3-codon partitioned ML analysis was also conducted in IQ Tree). For each ML analysis, 10 runs and a thorough bootstrapping (1000 replicates) was used to assess node support. Since topologies and support were identical for all nucleotide datasets (original, first/second and third codon position partitioned, and separate codon partitions), Bayesian Inference (BI) analyses were conducted only with the original nucleotide and amino-acid-translated datasets, partitioned by gene. Bayesian Inference analyses were conducted with MrBayes v.3.2.7a (Huelsenbeck and Ronquist, 2001; Ronquist and Huelsenbeck, 2003). Since MrBayes was unable to incorporate the same models as RAxML-NG, the most similar model that could be accommodated by MrBayes was assigned to each gene partition instead (see Supplementary Table 3). For the amino-acid-translated dataset, a single fixed model was chosen for all amino-acid-translated partitions (MTMAM, based on the most frequent model chosen by ModelTest-NG), with the non-protein-coding genes assigned the same models as in the nucleotide-only analysis (Supplementary Table 3). For both the nucleotide and amino-acid-translated datasets, BI analyses were carried out with Markov chain Monte Carlo (MCMC) for 20 million generations with 4 chains and trees sampled every 1000 generations. Burn-in was determined to be 5% using Tracer v.1.7 (Rambaut et al., 2018). Maximum parsimony (MP) analyses were also conducted with PAUP* v.4.0a168 (Swofford, 2003) for the nucleotide and amino-acid-translated datasets using heuristic searches with the tree-bisection-reconnection branch-swapping algorithm and 1000 random addition replicates. For MP analyses, support values were determined with 1000 bootstrap replicates.

Since the nucleotide and amino-acid-translated datasets produced slightly different topologies regarding the reciprocal monophyly of *Alaysia* and *Arcovestia*, an approximately unbiased (AU) test (Shimodaira, 2002) was conducted to test whether the reciprocal monophyly of *Alaysia* and *Arcovestia* was significantly different than a paraphyletic *Alaysia*. For the nucleotide dataset, a constrained tree forcing paraphyly of *Alaysia* and *Arcovestia* (placing *Arcovestia* sister to *Alaysia solwarawarriors* sp. nov.) was made using Mesquite 3.70 (Maddison and Maddison, 2018) and RAxML-NG. The AU test was conducted in IQ-Tree v.1.6.12 (Chernomor et al., 2016) with 20,000 replicates to generate likelihood scores and p-values for the constrained and unconstrained (ML nucleotide) trees. For the amino-acid-translated dataset, a constrained tree forcing reciprocal monophyly of *Alaysia* and *Arcovestia* was made using Mesquite and RAxML-NG. An AU test was then conducted in IQ-Tree with 20,000 replicates for the constrained and unconstrained (ML amino-acid-translated) trees.

To test for substitution saturation in the third codon position of the protein-coding genes, the index of substitution saturation (I_{ss}) was assessed with DAMBE 5 (Xia, 2013), following the protocol laid out in Xia and Lemey (2012). Whole alignments of each protein-coding gene were assessed using the proportion of invariant sites calculated by ModelTest-NG first. The proportion of invariant sites was then calculated for third codon positions using the ML nucleotide tree for estimation in DAMBE 5. For each protein-coding gene, the whole alignment, the first and second codon positions, and the third codon position were tested for substitution saturation using the Xia et al. test (as in Xia and Lemey, 2012), and calculations of I_{ss} and I_{ssc} were compared to determine saturation. No genes were found to be saturated based on the first and second codon positions, which are generally conserved, or the whole alignment. For genes where the third codon position appeared to be saturated ($I_{ss} > I_{ssc}$), additional ML, BI, and MP analyses were conducted with the nucleotide dataset with those genes omitted from the analyses (all parameters for each analysis otherwise the same as the previous analyses of the nucleotide dataset).

Since the nucleotide and amino-acid-translated datasets produced a topology with a placement of *Riftia pachyptila* that differs from its placement in some recent studies, an approximately unbiased test was also conducted to test whether the alternative topology (grouping *Riftia pachyptila* with the other vent-endemic taxa) was not significantly different than the topology recovered in all ML, BI, and MP analyses in this study. A constrained tree placing *Riftia pachyptila* with the clade containing the other vent-endemic taxa (*Ridgeia*, *Tevnia*, *Oasisia*, *Alaysia*, *Arcovestia*) was made using Mesquite and RAxML-NG. The AU test was conducted with IQ-Tree with 20,000 replicates to generate likelihood scores for the constrained and unconstrained (ML nucleotide) trees.

An ancestral state reconstruction (ASR) of habitat was conducted utilizing the whole mitochondrial genome dataset (nucleotide) with the addition of COI (and 16S and 18S when possible) sequences from GenBank for the following taxa (for which whole mitochondrial genomes have not been sequenced): *Oasisia fujikurai* Miura and Kojima, 2006, *Escarpia laminata* Jones, 1985, *Escarpia southwardae* Andersen et al., 2004, *Lamellibrachia anaximandri* Southward, Andersen & Hourdez, 2011, and *Lamellibrachia juni* Miura and Kojima, 2006 (Table 2). Another Maximum Likelihood analysis was conducted in RAxML-NG with models re-assessed with ModelTest-NG for genes with new data (COI, 16S, 18S) (Supplementary Table 3). The ancestral state reconstruction was conducted using this ML topology (Supplementary Figure 1) and a matrix of habitat types (vent, seep, organic fall; used '&-coding' for taxa known to inhabit multiple environments). The outgroup *Sclerolinum brattstromi* Webb, 1964 was excluded from the ASR analysis. The ASR was conducted in RStudio using R v.4.1.3, and the packages phytools v.1.0–1 (Revell, 2012) and corHMM v.2.7 (Beaulieu et al., 2013) were used to fit hidden Markov models of discrete character evolution. The AIC criterion determined the best model, "ER" (all rates equal) for the reconstruction.

2.5. Phylogenetic analyses of Alaysia and Arcovestia

Separate phylogenetic analyses were conducted with the newly sequenced COI, 16S, and 18S data for *Alaysia spiralis*, *Arcovestia ivanovi*, the two putative new species of *Alaysia*, and previously sequenced *Alaysia* and *Arcovestia* data from GenBank (Table 2). This data was combined with sequences for outgroups *Tevnia jerichonana, Oasisia alvinae, and Ridgeia piscesae*, available on GenBank (Table 2). The outgroups chosen for phylogenetic analyses were informed by the placement of *Alaysia* and *Arcovestia* in the 16-gene analyses (nucleotide and amino-acid-translated datasets agreed). The COI, 16S, and 18S datasets were aligned separately with MAFFT and tested with ModelTest-NG for the best-fit models under the AICc prior to concatenating (models assigned to each partition are listed in Supplementary Table 3). A Maximum Likelihood analysis was conducted with RAxML-NG with each partition assigned its appropriate model from ModelTest-NG, and a thorough bootstrapping (1000 replicates) was used to assess node support. A Bayesian Inference analysis was conducted for the same concatenated dataset in MrBayes. Since MrBayes was unable to incorporate the same models as RAxML-NG, the most similar models that could be accommodated by MrBayes were assigned to each gene partition instead (see Supplementary Table 3). The BI analysis was carried

out with Markov chain Monte Carlo (MCMC) for 20 million generations with 4 chains and trees sampled every 1000 generations. Burn-in was determined to be 5% using Tracer. An additional ML analysis was run with the same models as those implemented in MrBayes to assess whether differences in topologies produced by the two analyses were due to model selection differences (same settings as previous ML analysis, except for each gene partition being assigned the same models as those used for the BI analysis). A Maximum Parsimony (MP) analysis was also conducted with PAUP* for the same concatenated dataset using heuristic searches with the tree-bisection-reconnection branch-swapping algorithm and 1000 random addition replicates. For the MP analysis, support values were determined with 1000 bootstrap replicates.

The newly generated COI sequences for *Alaysia* and *Arcovestia* from this study were combined with available *Alaysia* and *Arcovestia* GenBank sequences to calculate uncorrected and model-corrected inter- and intraspecific distances. For model-corrected distances for each species, models for each COI dataset (separated by species) were selected using the AICc criterion in jModelTest2 v.2.1.10 (Darriba et al., 2012) since PAUP* was unable to incorporate models from ModelTest-NG. Haplotype networks were also created using these COI datasets (terminals listed in Table 2) for *Alaysia spiralis*, *Arcovestia ivanovi*, *Alaysia* sp. nov. 1 and *Alaysia solwarawarriors* sp. nov. with PopART v.1.7 (Leigh and Bryant, 2015) the median-joining option and default settings (Bandelt et al., 1999). Owing to some short COI sequences limiting the total sequence alignment length for haplotype network analyses, multiple haplotype network versions were created with various alignment lengths (omitting sequences that were very short) for comparison (for the *Arcovestia ivanovi*, *Alaysia spiralis,* and *Alaysia solwarawarriors* sp. nov. networks; not necessary for the *Alaysia* sp. nov. 1 network since there were only three sequences of roughly equal length). Differences between networks were small, but side-by-side comparisons of each network are available in Supplementary Figure 2.

2.6. Divergence time estimation

The BEAST v2.7.4 package (Bouckaert et al., 2019) was used to assess the divergence times within Vestimentifera. The oldest reported fossils that have been reported as unequivocally belonging to Vestimentifera are from hydrothermal vents (Figueroa massive sulphide deposit) dating from the early Jurassic (Pliensbachian to Toarcian) ~ 183–193 million years ago (mya) (Little et al., 2004, Georgieva et al., 2019). Georgieva et al. (2019) found that the fossil Figueroa tubes nested among the extant vestimentiferan terminals they used in their cladistic of tube morphology. For this reason, we applied a node-based date constraint for crown Vestimentifera. BEAUti from the BEAST2 package was used with the following parameters: optimized relaxed clock, birth–death model of divergence, and a log normal age distribution for the crown Vestimentifera node with 95% of dates from 183 to 193 and a mean of 188 mya. We used the 13 protein-coding genes as nucleotides and the two mitochondrial RNA genes as separate partitions with the closest models available in BEAST2 to those chosen in ModelTest-NG as done for the MrBayes analysis. We did not include the 18S data owing since some terminals lack this dataset and it could not then be combined with the other partitions in BEAST2. BEAST2 executed the.xml file using a random starting tree with 20 million generations, and this was repeated to produce three separate MCMC analyses. Results were assessed for stationarity, convergence, and effective sample size with Tracer 1.7. The trees for the three runs (30% burn-in each) were combined with Log Combiner and Tree Annotator (both part of the BEAST2 package) was used to generate a maximum-clade credibility majority-rule consensus tree with mean ages for the unconstrained nodes.

3. Results

3.1. Mitochondrial genome sequencing and composition

Gene order was identical among the newly sequenced taxa (*Alaysia spiralis* and *Alaysia solwarawarriors* sp. nov., *Arcovestia ivanovi, Escarpia spicata* (Costa Rica) and *Escarpia spicata* (Gulf of Mexico), *Oasisia* sp. nov., *Lamellibrachia barhami, Lamellibrachia columna, Lamellibrachia donwalshi,* and *Riftia pachyptila*) and the available vestimentiferan mitochondrial genomes from GenBank. All genes were encoded on a single strand for each newly sequenced mitochondrial genome, which is consistent with previous reports for other members of Vestimentifera and common within Annelida (Boore, 1999; Li et al., 2015), see Table 1 for details. The newly sequenced mitochondrial genomes also had similar total lengths compared to previously sequenced mitochondrial genomes for other members of Vestimentifera, ranging from 14,981–16,566 bp (Table 1). AT and GC content were also like other Vestimentifera, ranging from 63.50% to 65.75% and 36.50%-34.35% respectively (Table 1). A putative control region was identified by locating a noncoding repetitive region in each mitochondrial genome between *trnR* and *trnH* (annotated by MITOS), which is also consistent with previously published mitochondrial genomes within Vestimentifera. Mitochondrial contigs generally started or stopped in this region, perhaps due to repetitive elements interfering with assembly (Nagarajan and Pop, 2013).

3.2. Sixteen-gene phylogenetic analyses

The 16-gene Maximum Likelihood (ML), Bayesian Inference (BI), and Maximum Parsimony (MP) analyses of both the nucleotide and amino-acid-translated datasets produced similar topologies with similarly high levels of support at most nodes (Fig. 3). All analyses of the nucleotide dataset (including those which partitioned the third codon position separately from the first and second positions in protein-coding genes) produced congruent topologies, and all analyses of the amino-acid-translated dataset produced congruent topologies (topologies produced from the nucleotide and amino-acid-translated datasets differed slightly from each other, discussed in additional detail below). All analyses of both datasets recovered well-supported clades of *Lamellibrachia*, *Escarpia* and *Oasisia*, and supported the *Lamellibrachia* clade as sister to the remaining Vestimentifera. All analyses also supported a clade of Pacific vent-endemic taxa (consisting of *Oasisia*, *Ridgeia*, *Tevnia*, *Alaysia*, and *Arcovestia*) that excluded *Riftia pachyptila. Riftia pachyptila* was instead placed sister to the remaining Vestimentifera (excluding *Lamellibrachia*) in all analyses. The placement of *Escarpia spicata* was also notable (and identical in all analyses). While two newly sequenced *Escarpia spicata* mitochondrial genomes, one from the Eastern Pacific off Costa Rica and one from the Gulf of Mexico, grouped together with a very short branch length, the existing mitochondrial genome referred to as *Escarpia spicata* from GenBank (also from the Gulf of Mexico; Li et al., 2015) was clearly separate from the others and is referred to here as *Escarpia "laminata"* (discussed in additional detail below).

As noted above, tree topologies differed slightly between the ML, BI, and MP analyses derived from the nucleotide dataset versus the analyses derived from the amino-acid-translated dataset. All analyses derived from the nucleotide dataset produced identical topologies in which *Alaysia* and *Arcovestia* were recovered as reciprocally monophyletic (Fig. 3). All analyses derived from the amino-acid-translated dataset produced congruent topologies in which *Alaysia* and *Arcovestia* were recovered as paraphyletic, with *Arcovestia* nested inside *Alaysia* (*Arcovestia* sister to *Alaysia solwarawarriors* sp. nov.) (Supplementary Figure 3). No other differences were observed between the tree topologies produced by the nucleotide and amino-acid-translated datasets.

Each protein-coding gene was tested for substitution saturation in DAMBE using the nucleotide alignment for that gene. Each nucleotide alignment was tested both as a whole alignment and at the third codon

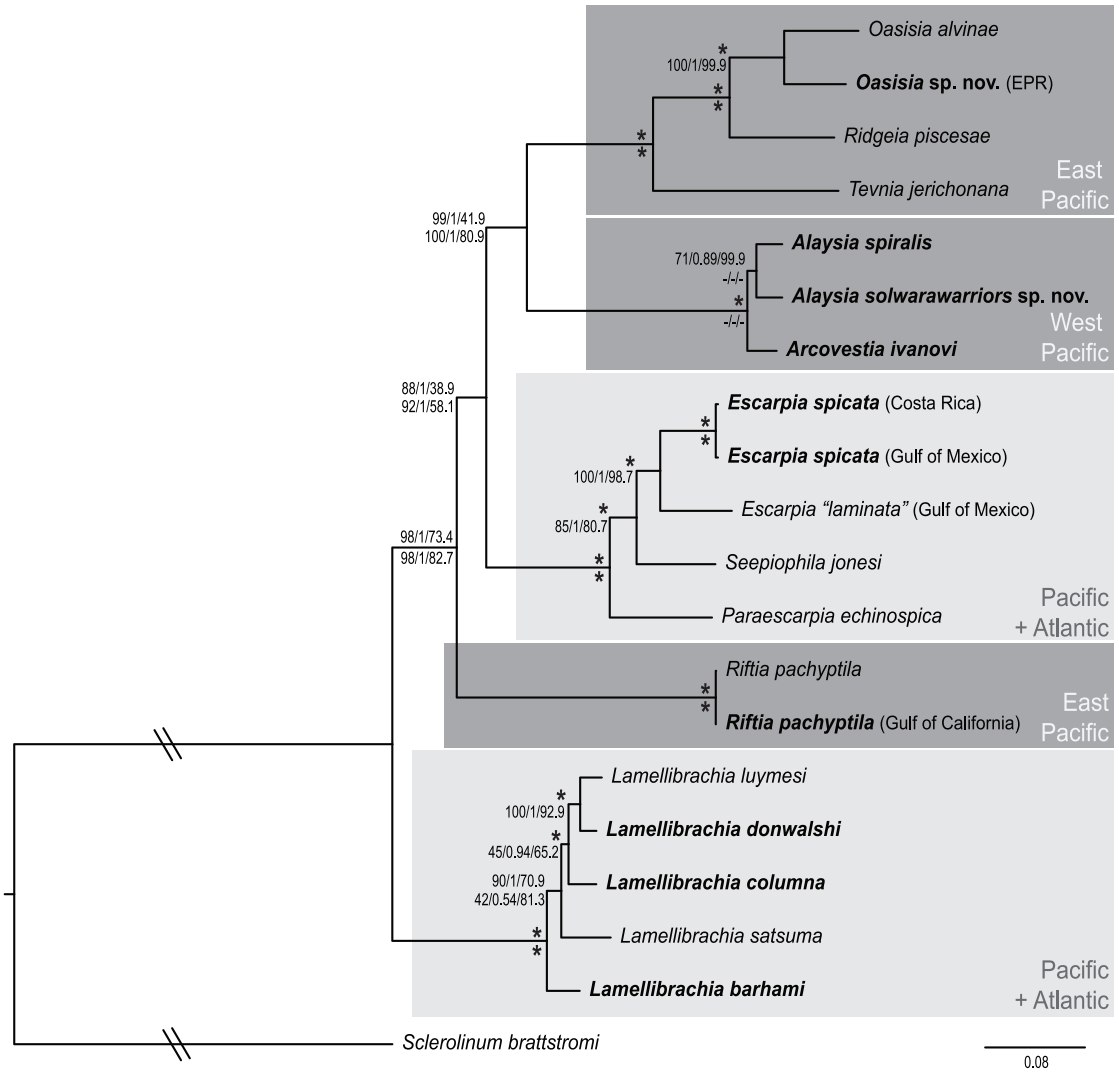

Fig. 3. Maximum Likelihood tree of the concatenated 16-gene nucleotide data. Support values above nodes are from nucleotide-only dataset, support values below nodes are from amino-acid-translated dataset. Bootstrap support percentages from the ML analysis are listed first, followed by Bayesian posterior probabilities and bootstrap support percentages from the Maximum Parsimony analysis. Stars indicate maximal support from all three analyses. Nodes not recovered by an analysis are indicated by a hyphen.

position to assess potential substitution saturation at that position (Table 4). Of the thirteen protein-coding genes, three exhibited an index of substitution saturation (I_{ss}) value that was significantly greater than the critical index of substitution saturation (I_{ssc}) value at the third codon position, thus indicating saturation in those genes (ATP8, ND4L, ND6). Additional ML, BI, and MP analyses of the nucleotide dataset excluding the saturated genes produced identical topologies to the original nucleotide dataset analyses (Supplementary Figure 4).

Since the potential reciprocal monophyly of *Alaysia* and *Arcovestia* differed between the nucleotide and amino-acid-translated datasets, an Approximately Unbiased (AU) test was conducted for each dataset to compare the two potential topologies. For the nucleotide dataset, the ML topology (Fig. 3, *Alaysia* and *Arcovestia* reciprocally monophyletic) was compared with a constrained tree in which *Alaysia* was paraphyletic (*Arcovestia* sister to *Alaysia solwarawarriors* sp. nov). The p-values for the ML (monophyly) and constrained (paraphyly) trees were not significantly different ($p = 0.122$). For the amino-acid-translated dataset, the ML topology (Supplementary Figure 3, *Alaysia* paraphyletic with *Arcovestia* sister to *Alaysia solwarawarriors* sp. nov.) was compared with a constrained tree in which *Alaysia* and *Arcovestia* were reciprocally monophyletic. Again, these were not significantly different ($p = 0.134$). Hence, neither AU test conducted in IQ-Tree recovered a significant difference in assessing if *Alaysia* was paraphyletic regarding *Arcovestia,* or if they can be accepted as reciprocally monophyletic genera.

The placement of *Riftia pachyptila* in this study differed from its placement in some other recent publications. An AU test was therefore also conducted to compare the topology recovered in this study with an alternative placement of *R. pachyptila* within the clade of Pacific vent-endemic taxa. The test compared the ML topology (Fig. 3) with a tree that constrained *R. pachyptila* within a clade of vent-endemic taxa (*Oasisia, Ridgeia, Tevnia, Alaysia, Arcovestia*). The AU test conducted in IQ-Tree did not recover a significant difference between the ML and constrained trees (p-value = 0.0767).

A likelihood ancestral state reconstruction (ASR) of habitat (vent, seep, and/or organic fall) was conducted on the ML tree topology (including additional vestimentiferan species with available GenBank data, not just those with whole mitochondrial genomes). The ASR revealed that a vent origin was most likely for the most recent common ancestor of the Vestimentifera clade. It also revealed two potential origins of seep-dwelling taxa: one for the *Lamellibrachia* clade and one leading to the most recent common ancestor of the *Paraescarpia* + *Seepiophila* + *Escarpia* clade (Fig. 4).

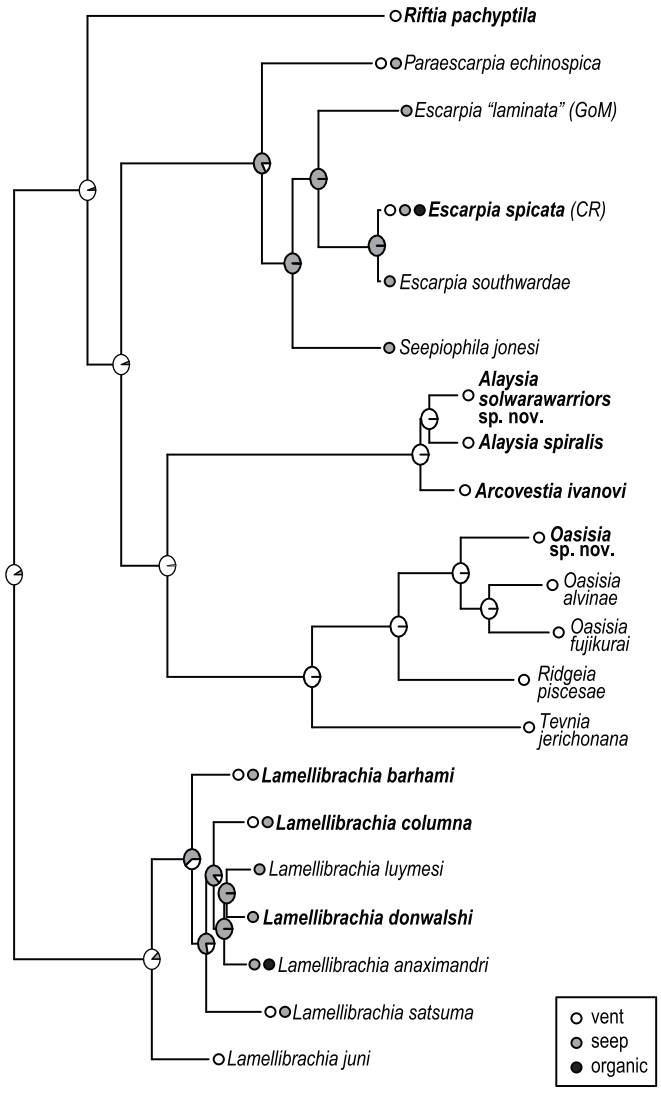

Fig. 4. Ancestral state reconstruction of habitat (vent, seep, organic fall) mapped onto the Maximum Likelihood phylogeny generated from the 16-gene concatenated nucleotide data with additional terminals (Supplementary Figure 1); outgroup not included in reconstruction.

The divergence time estimation for Vestimentifera (Supplementary Figure 6) had the split between *Lamellibrachia* and the remaining Vestimentifera constrained to the early Jurassic (~188 million years ago (mya) and age of the root, the split of Vestimentifera from *Sclerolinum*, was estimated to be in the Triassic at ~ 217 mya. The divergences within *Lamellibrachia* all occurring during the Cenozoic, in the last 50 mya. The split between the sister species pair *L. luymesi* and *L. donwalshi*, which live in the Gulf of Mexico/Caribbean and eastern Pacific respectively, was recovered as having occurred ~ 15 mya. In the other clade comprising the remaining Vestimentifera, *Riftia* diverged from the remaining terminals in the late Jurassic (~160 mya) with all the other divergences happening in the Cretaceous to Cenozoic. The *Arcovestia/Alaysia* clades was found to date back 30 mya, with the split between *Alaysia spiralis* and *Alaysia solwarawarriors* sp. nov. dating to ~ 19 mya.

3.3. Three-gene phylogenetic analyses of Alaysia and Arcovestia

Phylogenetic analyses of *Alaysia* and *Arcovestia* were also conducted with a three-gene (COI, 16S, 18S) concatenated dataset. While various outgroup choices for the concatenated three-gene phylogenetic analyses resulted in differing topologies with varied and poor support, the results of the much larger 16-gene datasets placed the *Alaysia* + *Arcovestia* clade sister to the vent-endemic taxa *Tevnia jerichonana*, *Oasisia alvinae*, and *Ridgeia piscesae* regardless of the dataset used. Based on this result, all three of these vent-endemic taxa were chosen as outgroups for the three-gene phylogeny of *Alaysia* and *Arcovestia*. The ML, BI, and MP analyses of this concatenated three-gene dataset all consistently recovered *Alaysia spiralis* as sister to *Alaysia* sp. A3 with a very short branch length (Fig. 5). These and other phylogenetic analyses (see below) indicate that *Alaysia* sp. A3 is *Alaysia spiralis*. At the time of its publication, there was not molecular data available for *A. spiralis*, so it was tentatively referred to as *Alaysia* sp. A3 (Kojima et al., 2003). The *A. spiralis* clade was also recovered by all analyses to be sister to a clade consisting of *Alaysia* sp. A1 and *Alaysia* sp. A2. However, the remaining terminals varied in position between analyses, and many relationships within the trees were poorly supported (Fig. 5, Supplementary Figure 5). The ML analysis (Fig. 5, Supplementary Figure 5A) produced a topology with reciprocally monophyletic *Alaysia and Arcovestia* clades. Within the *Alaysia* clade, *Alaysia solwarawarriors* sp. nov. was placed sister to *Alaysia* sp. A4 (from the Mid Okinawa Trough) and *Alaysia* sp. nov. 1 was placed sister to the remaining *Alaysia* species (*Alaysia spiralis, A.* sp. A1, *A.* sp. A2, and *A.* sp. A3). The BI analysis (Supplementary Figure 5B) also recovered a clade that included *Alaysia spiralis, A.* sp. A1, *A.* sp. A2, and *A.* sp. A3. However, the BI analyses did not recover reciprocally monophyletic *Alaysia* and *Arcovestia* clades. Instead, *Arcovestia ivanovi* was nested inside a grade of *Alaysia* species (Supplementary Figure 5B). An additional ML analysis of the same dataset with the same models that were applied in MrBayes (instead of those chosen by ModelTest-NG and implemented in RAxML-NG) resulted in the same topology as the BI analysis. The MP analysis (Supplementary Figure 5C) also recovered a clade containing *Alaysia spiralis, A.* sp. A1, *A.* sp. A2, and *A.* sp. A3. However, while the MP analysis did also recover a grade of *Alaysia* species with *Arcovestia ivanovi* nested inside, as in the BI analysis, the placement of the various *Alaysia* species in this grade in the MP analysis differed from that of the BI analysis (Supplementary Figure 5B, 5C).

An uncorrected pairwise distance analysis for the COI dataset revealed low intraspecific distances within *Alaysia* and *Arcovestia*, with maximum intraspecific distances ranging from 0.09% (*Alaysia solwarawarriors* sp. nov.) to 1.39% (*Arcovestia ivanovi*) (Table 3, Supplementary Table 2). Corrected intraspecific distances for each species revealed similar results (*Alaysia solwarawarriors* sp. nov.: 0–0.09%, *Alaysia* sp. nov. 1: 0.31–0.64%, *Alaysia spiralis:* 0–1.37%, *Arcovestia ivanovi:* 0–1.47%). The minimum interspecific pairwise distance between *Arcovestia ivanovi* and *Alaysia spiralis* was 4.51% (uncorrected) to 5.84% (corrected). The minimum interspecific pairwise distance between *Alaysia spiralis* and *Alaysia* sp. A3 was 0.10% (uncorrected and corrected), which also supports the conclusion that *Alaysia* sp. A3 is *A. spiralis*. The minimum interspecific distance between *A. spiralis* and its closest relative, *Alaysia* sp. A1, was 2.48% (uncorrected) to 2.81% (corrected). The minimum interspecific pairwise distance between *Alaysia solwarawarriors* sp. nov. and its closest relative, *Alaysia* sp. A4, was 3.38% (uncorrected) to 3.86% (corrected). The minimum interspecific pairwise distance between *Alaysia* sp. nov. 1 and its closest relative, *Alaysia* sp. A1, was 6.02% (uncorrected) to 8.22% (corrected).

Haplotype networks generated for the COI dataset revealed low haplotype diversity within the species for which multiple COI sequences were available (Fig. 6). Because missing data could not be accommodated in haplotype network analyses, multiple networks were created to compare haplotype diversity with various total alignment lengths for comparison (excluding taxa with short sequences as needed). The differences between these networks were negligible (Supplementary Figure 2), and the networks with the greatest haplotype diversity are shown in Fig. 6. The majority of *Arcovestia ivanovi* specimens (Fig. 6A) specimens shared a single haplotype regardless of locality and differed by up to 5 base pairs. *Alaysia spiralis* (Fig. 6B) specimens followed a similar pattern with a single common haplotype, with a specimen from the type locality differing from the most common haplotype by 3 base

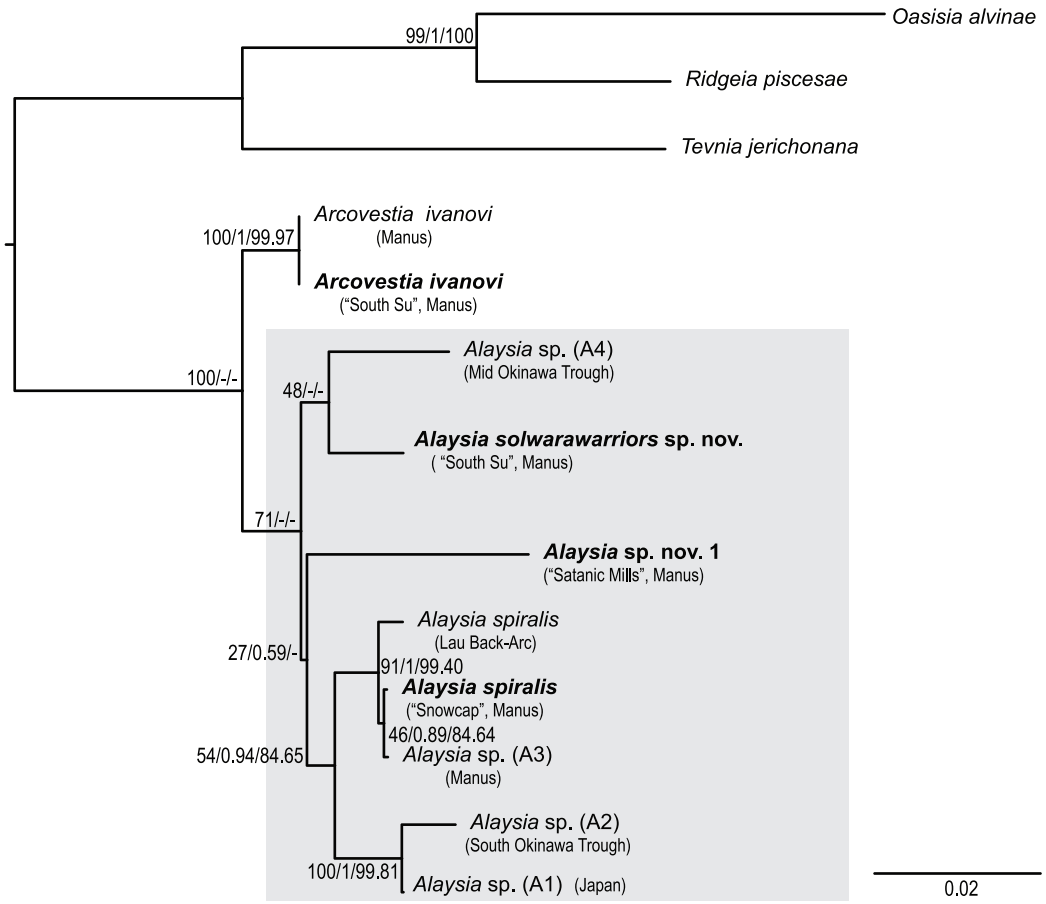

Fig. 5. Maximum Likelihood tree of the concatenated three-gene nucleotide data. Bootstrap support percentages from the ML analysis are listed first, followed by Bayesian posterior probabilities and bootstrap support percentages from the Maximum Parsimony analysis. Nodes not recovered by an analysis are indicated by a hyphen. *Alaysia* clade highlighted in grey.

Table 3
Summary of uncorrected and corrected pairwise distances for *Alaysia* and *Arcovestia* COI data. Model listed for corrected pairwise distances.

TAXA	MODEL	MINIMUM INTRASPECIFIC DISTANCE		MAXIMUM INTRASPECIFIC DISTANCE		MINIMUM INTERSPECIFIC DISTANCE	
Species	**For Corrected Analyses**	**Uncorrected**	**Corrected**	**Uncorrected**	**Corrected**	**Uncorrected**	**Closest Taxon**
Arcovestia ivanovi	HKY	0	0	1.39%	1.47%	4.51%	*Alaysia spiralis*
Alaysia spiralis	HKY	0	0	1.24%	1.37%	2.48%	*Alaysia* sp. A1
Alaysia solwarawarriors sp. nov.	F81	0	0	0.09%	0.09%	3.38%	*Alaysia* sp. A4
Alaysia sp. nov. 1	HKY	0.31%	0.31%	0.62%	0.64%	6.02%	*Alaysia* sp. A1
Alaysia sp. A1	–	–	–	–	–	1.28%	*Alaysia* sp. A2
Alaysia sp. A3	–	–	–	–	–	0.10%	*Alaysia spiralis*

pairs. *Alaysia solwarawarriors* sp. nov. (Fig. 6C) showed the lowest haplotype diversity (just a single haplotype for the 10 specimens sequenced) and *Alaysia* sp. nov. 1 (Fig. 6D) also showed relatively low haplotype diversity, with specimens differing by at most 4 base pairs (note that the number of specimens sequenced for *Alaysia* sp. nov. 1 was lower than for the other species).

4. Taxonomy

4.1. Family - Siboglinidae Caullery, 1914

Alaysia Southward, 1991

Diagnosis.

Characterized by the possession of outer lamellar sheaths, a smooth obturacular face, absence of axial rod, presence of dorsal groove in obturacular stalk, and an entire posterior vestimental fold.

Type species: *Alaysia spiralis* Southward, 1991.

4.2. Alaysia solwarawarriors sp. nov.

urn:lsid:zoobank.org:pub:D845ED8D-C188-4E7E-A4B7-05BB908D9DD3.

(Fig. 7).

4.2.1. Type locality

Manus Basin, vent site known as "South Su", approximately 1,452 m depth; −3.811 S, 152.103 E.

4.2.2. Material examined

Holotype: SIO-BIC A14168 (1 individual), collected on April 15,

Table 4
Index of substitution saturation (I_{ss}) and critical index of substitution saturation I_{ssc}) values for third codon position and whole alignments of protein-coding genes. Bold values are significant (p-value less than 0.05).

	Position 3		Whole Alignment	
Gene	I_{ss}	I_{ssc} (Sym)	I_{ss}	I_{ssc} (Sym)
ATP6	0.6484	0.6247	0.5003	**0.743**
ATP8	0.6466	**0.3209**	0.5067	0.5693
COX1	0.5361	**0.7167**	0.4482	**0.7853**
COX2	0.5172	**0.6247**	0.4304	**0.743**
COX3	0.5933	0.6416	0.4461	**0.7519**
CYTB	0.6171	**0.6858**	0.469	**0.7725**
ND1	0.5976	**0.6629**	0.4703	**0.7621**
ND2	0.6357	0.6669	0.4969	**0.7639**
ND3	0.5389	**0.6748**	0.5182	**0.6748**
ND4L	0.6325	**0.4751**	0.4715	**0.6557**
ND4	0.6113	**0.7023**	0.4986	**0.7799**
ND5	0.6284	**0.7259**	0.4932	**0.7877**
ND6	0.6434	**0.5672**	0.509	**0.707**

2007, from "South Su" vent site, Manus Basin at 1,452 m depth; −3.811 S, 152.103 E. Collected by Patrick Collins and Carol Logan. Fixed and preserved whole (within chitinous tubes) in 95% ethanol.

Paratypes: SIO-BIC A14167A-N (14 specimens), collected on April 15, 2007, from "South Su" vent site, Manus Basin at 1,452 m depth; −3.811 S, 152.103 E. Collected by Patrick Collins and Cindy Van Dover. Fixed and preserved whole (within chitinous tubes) in 95% ethanol. Type and voucher material is held at the Scripps Institution of Oceanography Benthic Invertebrate Collection (SIO-BIC), La Jolla, California, or South Australian Museum (SAM), Adelaide, South Australia.

4.2.3. Description

Anterior crown (branchial plume) plus obturaculum length of holotype 1.0 mm, crown diameter 1.0 mm. Vestimentum length 1.0 cm, vestimentum diameter ~ 1.0 mm (Fig. 7A, G7B). Obturaculum with dorsal groove and slightly cup-shaped top. Outer sheath lamellae emerge from vestimentum in a pair, clear median split with no lamellae at the center of the dorsal side, obturaculum visible through that split (Fig. 7C, Fig. 7D). Branchial lamellae also emerge from vestimentum and appear to be fused at the base, with a longer free portion at the anterior tip with pinnules (Fig. 7D). Paired genital grooves appear to run the length of the vestimentum on the dorsal side (Fig. 7A, Fig. 7C). Outer surface of vestimentum and trunk are dotted with small papillae likely carrying cuticular plaques (Fig. 7E, Fig. 7F). All specimens incomplete, lacking opisthosoma. Tubes observed for holotype and multiple paratypes. Tubes are smooth and stiff, often semi-transparent (Fig. 7G). Anterior part of tube is often curved or coiled (Fig. 7G). Tube is thin and appears to lack distinct collars, approximate diameter (holotype) 1.1 mm, approximate length 12.1 cm.

4.2.4. Etymology

Alaysia solwarawarriors sp. nov. is here named in collaboration with Jonathan Mesulam and the Alliance of Solwara Warriors. The name is intended to honor the Alliance of Solwara Warriors for their critical role in protecting the deep-sea ecosystems of the region, as well as the environmental and cultural interests of local communities in Papua New Guinea and the surrounding provinces.

4.2.5. Distribution

Alaysia solwarawarriors sp. nov. has been recovered from two diffuse flow vent sites in proximity in the Manus Basin (within 0.083 decimal degrees of latitude and 0.434 decimal degrees of longitude).

4.2.6. Remarks

Alaysia solwarawarriors sp. nov. has notable similarities to the type species *Alaysia spiralis*, including similar shape/size of obturaculum with dorsal groove, similar arrangement of branchial and sheath lamellae, presence of paired genital grooves on the dorsal side of the vestimentum, small papillae on the vestimentum and trunk, spiraling of the tube, and absence of an axial rod. However, the *Alaysia solwarawarriors* sp. nov. holotype appears to have a smaller crown and vestimentum diameter, and tubes of holotypes and paratypes are curved but not always as coiled like a corkscrew as in the original description of *A. spiralis* (E. C. Southward, 1991). *Alaysia solwarawarriors* sp. nov. differs genetically from *Alaysia spiralis* and other currently undescribed new species of *Alaysia*.

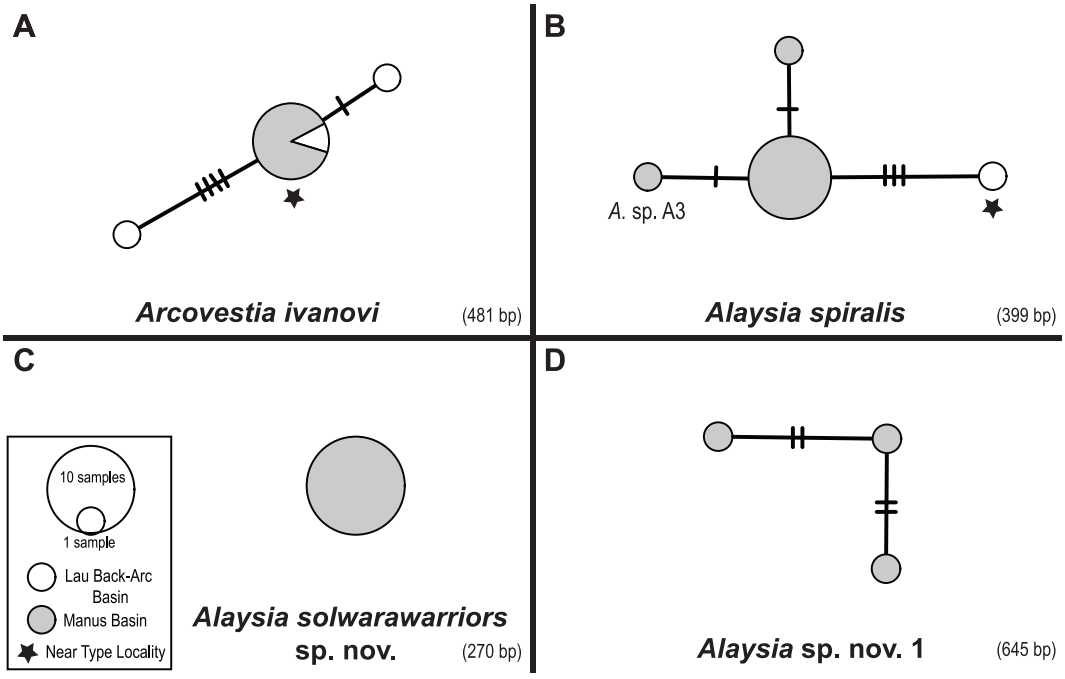

Fig. 6. Haplotype networks from COI data for (A) *Arcovestia ivanovi*, (B) *Alaysia spiralis*, (C) *Alaysia solwarawarriors* sp. nov., and (D) *Alaysia* sp. nov. 1. Color-coded according to locality.

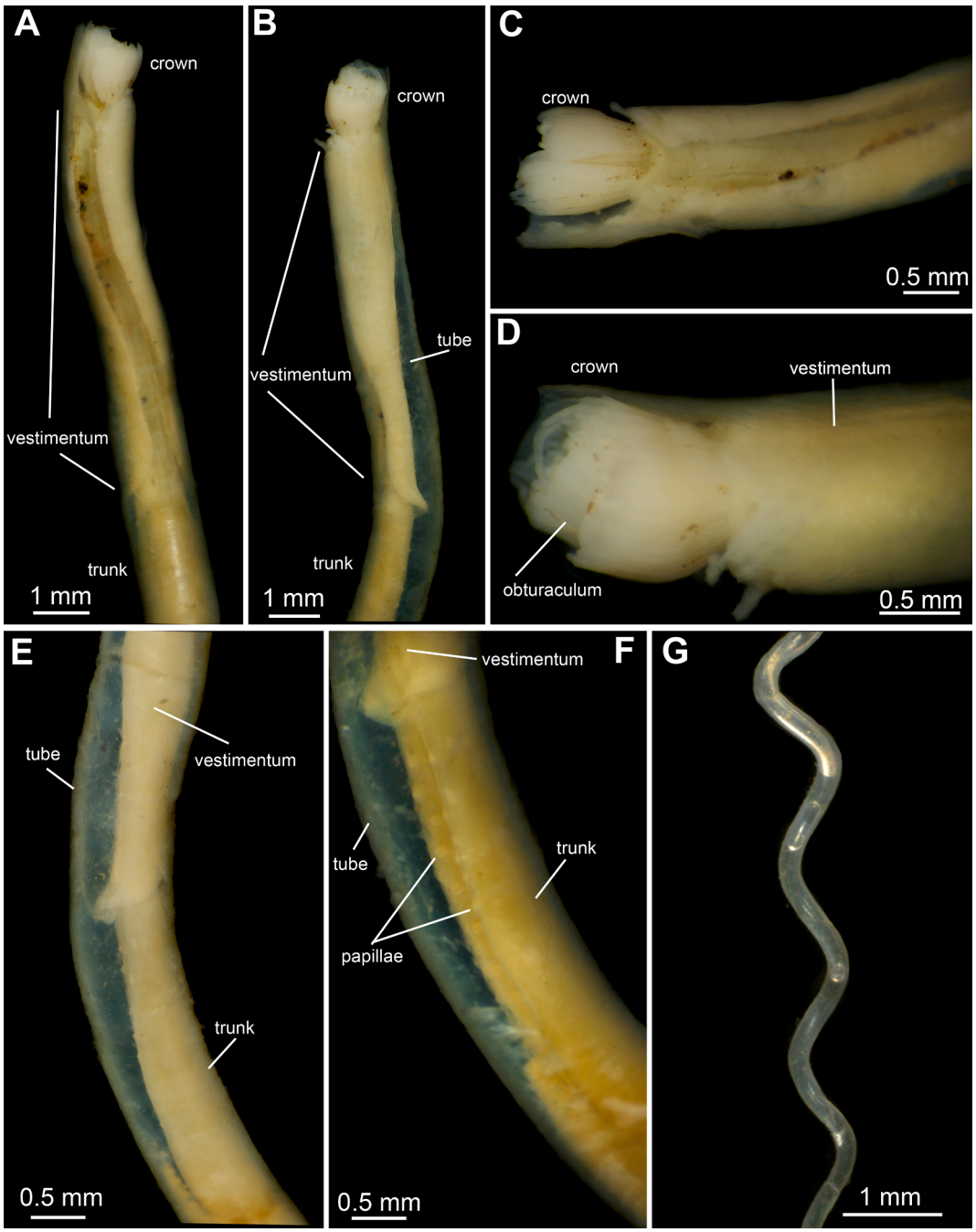

Fig. 7. Photographs of *Alaysia solwarawarriors* sp. nov. (SIO-BIC A14168). (A) Dorsal anterior. (B) Lateral anterior. (C) Close-up of dorsal anterior. (D) Close-up of lateral anterior. (E) close-up of lateral vestimentum and trunk. (F) close-up of trunk. (G) chitinous tube.

5. Discussion

5.1. Sixteen-gene phylogenetic analyses

This study provides the most complete mitogenomic phylogeny of Vestimentifera to date, with ten new mitochondrial genomes and nuclear 18S included and including representatives of all genera. All analyses (Maximum Likelihood, Bayesian Inference, and Maximum Parsimony) of both nucleotide and amino-acid-translated datasets show very similar topologies and high support at most nodes. Similar topologies have been found in previous studies (Li et al., 2015, 2017; Patra et al., 2016) with some differences in the placement of *Riftia pachyptila* (Li et al., 2015, 2017; Sun et al., 2018), which will be discussed in more detail below. All analyses recovered well-supported monophyletic clades of *Lamellibrachia, Escarpia,* and *Oasisia*, with the *Lamellibrachia* clade recovered as sister to the remaining Vestimentifera. This result is consistent with all recent phylogenies of Vestimentifera that utilize whole mitochondrial genome data and/or transcriptome data (Li et al., 2015, 2017; Patra et al., 2016; Sun et al., 2018). The placement of various *Escarpia spicata* terminals calls into question the identification of the *E. spicata* specimen available on GenBank from the Gulf of Mexico. The type locality of *E. spicata* lies in the eastern Pacific, off the Mexico/USA border (Jones, 1985) and there is genetic data from near this locality (GenBank accession number U84262); therefore, it seems most likely that the *E. spicata* specimen from Costa Rica (also from the East Pacific) is a true *E. spicata*. The previously identified *E. spicata* specimen from the Gulf of Mexico, which is separated by a considerable branch length from the Costa Rica *E. spicata,* may therefore be *E. laminata*,

which has been morphologically identified in the Gulf of Mexico (Cowart et al., 2013). The terminal is labeled here as *E. "laminata"* (Fig. 3) indicating the uncertainty of its identity until it can be confirmed with morphological or additional molecular data (morphological data and/or a voucher specimen associated with this sequence were not reported by Li et al. (2015). The potential identification of this specimen as *E. laminata* is further corroborated by the additionally sequenced *E. spicata* specimen from the Gulf of Mexico from this study, which clearly groups with the *E. spicata* from Costa Rica, suggesting this species has a very wide distribution.

This study places *Alaysia* and *Arcovestia* within the larger Vestimentifera phylogeny for the first time. While the placement of these taxa as sister taxa to each other and as forming a clade that is sister to the other Pacific vent-endemic taxa *Oasisia, Ridgeia,* and *Tevnia* is well-supported in all analyses, the reciprocal monophyly of *Alaysia* and *Arcovestia* varied between the nucleotide and amino-acid translated datasets. The Approximately Unbiased (AU) tests conducted for the nucleotide and amino-acid-translated datasets to compare these two possible topologies (reciprocally monophyletic versus paraphyletic *Alaysia*) did not produce any significant results. Tests for substitution saturation in DAMBE (Table 4) revealed three potentially saturated genes in the dataset, so phylogenetic analyses (ML, BI, MP) were repeated with those genes (ATP8, ND4L, ND6) removed. The analyses produced phylogenies identical to the original nucleotide analyses, indicating that saturation was not the cause of the differing topologies. This is unsurprising given that substitution saturation is often suggested to affect mostly deep nodes and branches in a phylogeny (Xia and Lemey, 2012) as has been shown in some major arthropod groups (Xia et al., 2003), while the relationship between *Alaysia* and *Arcovestia* is fairly shallow in this phylogeny. Given that some clades within Vestimentifera, such as *Escarpia* and *Lamellibrachia* have been known to exhibit low diversity in various mitochondrial and nuclear genes such as COI, cytochrome *B*, and 18S (Cowart et al., 2013; Miglietta et al., 2010), and exhibit small genetic distances between species (Cowart et al., 2013; McCowin et al., 2019; Miglietta et al., 2010), it may be possible that the already limited phylogenetic signal in the nucleotide data is being lost in the amino-acid-translated dataset for *Alaysia* and *Arcovestia*. If this is the case, the nucleotide dataset and phylogeny may be a more accurate representation of the data until more nuclear loci can be obtained for *Alaysia* and *Arcovestia*. The original description of *Arcovestia ivanovi* placed *Alaysia* and *Arcovestia* into separate families due to their morphological differences (e.g. presence/absence of outer sheath lamellae) (Southward and Galkin, 1997). While these families are now synonymized under Siboglinidae, the morphological differences between *Alaysia* and *Arcovestia* remain. Given the current molecular data and morphological evidence, we therefore maintain *Alasyia* and *Arcovestia* as separate genera.

While the 16-gene analyses in this study produced topologies that are similar to multiple previous studies utilizing similar datasets (Li et al., 2017, 2015; Patra et al., 2016), some studies report a notable difference in the placement of *Riftia pachyptila* (Li et al., 2017, 2015; Sun et al., 2018). Those studies report *R. pachyptila* as sister to the other vent-endemic taxa, a contrast to the result in this study that placed *R. pachyptila* sister to a clade composed of the rest of the Vestimentifera (excluding *Lamellibrachia)*. Past studies often report middling support for the placement of *R. pachyptila*, regardless of its placement in the phylogeny (Li et al., 2017, 2015; Patra et al., 2016), while its placement away from the other vent-endemic taxa in this study is well-supported. Interestingly, this placement may be supported by morphological data. Jones (1988) noted some major morphological differences between *R. pachyptila* and the other vent endemic taxa, and he proposed that *Riftia* was sister to the remaining Vestimentifera (Jones, 1988). He noted such morphological differences as the locations of afferent and efferent plume vessels and branchial lamellae (axial in *R. pachyptila* and basally situated in all other Vestimentifera), the composition of dorsal and ventral mesenteries (separated by a central structure containing gonad and trophosome in *R. pachyptila*, containing major longitudinal blood vessels in other Vestimentifera), and *Riftia*'s particularly large size compared to other members of Vestimentifera (Jones, 1988). However, *R. pachyptila* does share some morphological traits with the other vent-endemic taxa as well, such as paired excretory pores (Jones, 1988). An AU test was conducted to assess whether the topology recovered by this study was better supported than a constrained topology in which *R. pachyptila* is forced to remain in a clade with the other vent-endemic Vestimentifera. Though the AU test did not produce significant results, the constrained result's likelihood was close to the unconstrainted (ML) tree (p-value = 0.0767). This study and much of the past literature relies heavily on mitochondrial markers for its phylogenetic conclusions, so further analyses with more data, including nuclear markers and transcriptome data (which Li et al. (2017) have shown to be effective in elucidating relationships among some Siboglinids) are desirable to remove ambiguity about the placement of *R. pachyptila* within Vestimentifera. However, both the phylogenetic evidence from this study and morphological evidence from past studies point away from a strong affinity between *R. pachyptila* and the other vent-endemic members of Vestimentifera.

The phylogenetic tree topology recovered by the 16-gene analyses in this study has interesting implications for the ancestral habitat of Vestimentifera. The likelihood ancestral state reconstruction (ASR) based on the maximum likelihood nucleotide phylogeny (that placed *Lamellibrachia* sister to all remaining Vestimentifera, followed by *Riftia* as sister to the rest) suggested that a vent origin was most likely for the most recent common ancestor of Vestimentifera, and this is supported by the first known vestimentiferan fossils dating to Jurassic hydrothermal vents (Little et al. 2004; Georgieva et al. 2019). This contrasts with Black et al.'s (1997) hypothesis that a seep Vestimentifera ancestor invaded vents, which was based on a tree topology that depicted a grade of seep to vent Vestimentifera. Past studies that showed conflicting topologies were often not well-supported, but the now well-supported phylogeny and ASR from this study suggest a vent ancestral origin for the whole group. In addition, the ASR shows two potential origins of seep taxa within Vestimentifera. One potential seep origin occurs at the most recent common ancestor for the clade composed of *Escarpia, Paraescarpia*, and *Seepiophila*, and one potential seep origin occurs within the *Lamellibrachia* clade (after *Lamellibrachia juni* diverged from the other *Lamellibrachia* species). When considering the biogeography of this group, a Pacific origin seems likely given that all major clades include at least some Pacific-dwelling taxa (Fig. 3). However, none of the vent-endemic taxa of the Pacific (including *Riftia*) have been reported from vents in any other oceans. Some taxa in the Atlantic are known to inhabit multiple habitats including vents, such as various *Lamellibrachia* species, but no Atlantic taxa are known only from vents. *Lamellibrachia* sp. 2, which has been noted from both seeps in the Gulf of Mexico and vents in the Caribbean at the Mid-Cayman Rise (Plouviez et al., 2014), is likely an example of a secondary colonization of vents. *Paraescarpia echinospica* Southward et al., 2002 is the only vestimentiferan species known to inhabit seeps in the Indian Ocean (Java Trench) and has been reported from both vents and seeps in the Pacific (originally as tentative species *Escarpia* sp. E2 by Kojima et al. in 2002, later identified as *Paraescarpia echinospica* by Kojima et al. in 2003). We therefore hypothesize that an ancestral Pacific/vent Vestimentifera colonized seeps and dispersed across the Atlantic Ocean, perhaps through the South American Seaway prior to the closure of the Panama Isthmus.

The divergence time estimation for Vestimentifera shown here (Supplementary Figure 6) is the first to use an age of the early Jurassic for the clade. This was enabled owing to a recent analysis of morphology by Georgieva et al. (2019) that confirmed fossils described by Little et al. (2004) as being part of the crown group. The only other study to date to use a fossil-based constraint for Vestimentifera was by Taboada et al. (2015), which used a stem-based constraint for two terminals of Vestimentifera dated at ~ 91 million years ago (mya) as the split from *Sclerolinum*. This was for their analysis of the divergence within *Osedax*.

Their constraint was based on late Cretaceous fossils from Little et al. (1999). This gave a timing for the split between *Lamellibrachia barhami* and *Riftia pachyptila* as ~ 80 mya. Our constrained date and the inferred phylogeny would place this divergence at 188 mya (Supplementary Figure 6) and the inferred split from *Sclerolinum* was in the Triassic at ~ 217 mya. Other estimations of the age and divergences within Vestimentifera have been based on rates of molecular evolution. These studies argued strongly against a Paleozoic origin for the group, which had been postulated based on fossils (see Little and Vrijenhoek 2003). Vrijenhoek (2013) summarized these molecular estimates and argued that the age of crown Vestimentifera was around 55 mya with the age for the split from other siboglinids at ~ 100 mya and argued against the Jurassic fossils as belonging to Vestimentifera. A reassessment of the rates of molecular evolution for Vestimentifera and calibration of clock rates that have been used previously (see Vrijenhoek 2013) may be warranted. The split shown here between the sister species pair of *Lamellibrachia donwalshi* and *L. luymesi*, which are separated by central America, dates to ~ 15 mya (Supplementary Figure 6). This is consistent with the vicariant separation of deep-water taxa such as these as the Panama Isthmus began to shoal (see Stiller et al. 2013).

5.2. Three-gene phylogenetic analyses of Alaysia and Arcovestia

The three-gene (COI, 16S, 18S) phylogenetic analyses (ML, BI, MP) of *Alaysia* and *Arcovestia* (Fig. 5) showed a well-supported close relationship between *Alaysia spiralis* and *Alaysia* sp. A3 (with a very short branch length) in all analyses, plus a very small intraspecific distance (0.10%) between the two terminals, indicating that the two are conspecific. This small distance between *A. spiralis* and *A.* sp. A3 is also displayed in the haplotype networks (Fig. 6B: 1 bp between *A.* sp. A3 and other *A. spiralis* specimens, and 4 bp between *A.* sp. A3 and *A. spiralis* from near the type locality). Neither morphological analyses nor vouchers of *A.* sp. A3 were provided by Kojima et al. (2003), but all molecular evidence (branch lengths, distances, networks) support *A.* sp. A3 as another *A. spiralis* specimen. All analyses also consistently recovered *A. spiralis* (+*A.* sp. A3) as sister to a clade consisting of *Alaysia* sp. A1 and *Alaysia* sp. A2. *Alaysia* sp. A1 is of particular interest as it was reported by Kojima et al. (2003) to be from a seep off Hatsushima Island (Japan) and may therefore represent the first *Alaysia* record from a seep. All analyses (including distances and networks) also supported the inclusions of *Arcovestia ivanovi* and *Alaysia spiralis* samples from outside their type localities within their respective species (Figs. 5, 6, and Supplementary Table 2).

The remaining nodes recovered by these ML, BI, and MP analyses seemed unstable and not well-supported, differing widely by method (Fig. 5, Supplementary Figure 5). While the ML analysis recovered reciprocally monophyletic *Alaysia* and *Arcovestia* clades, neither the BI nor the MP analyses did. However, it should be noted that the ML analysis implemented more nuanced models (e.g., more substitution schemes) than the BI analysis, and when reduced to the same simpler models as the BI analysis, produced an identical topology to the BI analysis. The MP analysis produced a different topology altogether, with very poor support, especially at nodes that differed from the other two analyses (Supplementary Figure 5). While the original ML analysis of this dataset still has some poorly supported nodes, given that the models implemented are likely an improvement on the other two analyses and the result matches the well-supported 16-gene nucleotide phylogeny, the ML analysis is likely the best hypothesis for the relationships between various *Alaysia* species and *Arcovestia ivanovi* given the available data.

While the three-gene phylogenetic analyses are not particularly well-supported at all nodes, there is still clear support for the existence of two new *Alaysia* species, *Alaysia* sp. nov. 1 and *Alaysia solwarawarriors* sp. nov. Branch lengths between the new species and their closest relatives are like those between other *Alaysia* species (Fig. 5). Additionally, minimum uncorrected pairwise distances between the two new *Alaysia* species and their respective closest relatives are similar to or larger than the distances between other putative new *Alaysia* species, excluding *A.* sp. A3 (Kojima et al., 2003, 2002). *Alaysia solwarawarriors* sp. nov. has a minimum distance of 3.38% from its closest relative, *A.* sp. A4 (and 4.51% to *A. spiralis*), and *A.* sp. nov. 1 has a minimum distance of 6.02% to its closest relative, *Alaysia* sp. A1 (Table 3, Supplementary Table 2). While interspecific distances are low, they are on par or larger than those exhibited by different species in other vestimentiferan genera, such as *Lamellibrachia* (distances on the order of 2% accepted between species) and *Escarpia* (Cowart et al., 2013; McCowin and Rouse, 2018). There also appears to be a clear gap between maximum intraspecific and minimum interspecific distances within the new *Alaysia* species: maximum uncorrected distances within each new species are very low (less than 1%, which is slightly less than the variation within *Alaysia* (maximum corrected distances of up to 1.37%). While exact placement of the new species within the *Alaysia* phylogeny is poorly supported and may change with additional data, all molecular data still supports the existence of two new species from the Manus Basin.

6. Conclusions

This study provides the most complete mitogenomic phylogeny of Vestimentifera to date, with the addition of ten newly sequenced mitochondrial genomes, including those for *Alaysia spiralis* and *Arcovestia ivanovi*, for which very little genetic data has been previously available. While the phylogenetic analyses presented in this study are largely consistent with other recent mitogenomic analyses of this group, the placement of *Riftia pachyptila* as sister to the rest of the Vestimentifera (excluding *Lamellibrachia*) with high support is notable. This placement has major implications for the habitat evolution of Vestimentifera, as a likelihood ancestral state reconstruction suggests that the most recent common ancestor of all Vestimentifera inhabited vents. However, it should be noted that this study relies heavily on mitochondrial markers due to the scarcity of available nuclear data, and its findings should be corroborated by additional (nuclear) markers in the future.

A new species of *Alaysia*, *Alaysia solwarawarriors* sp. nov. is also described from the Manus Basin, and molecular data is provided for another putative new species from the same area. The presence of multiple new species in an area previously slated for deep-sea mining highlights the importance of collecting biodiversity data in the deep sea. While mining companies have supported some biodiversity research in areas of interest, many putative new species from this region remain undescribed and there is still a dearth of detailed community structure data. Without this crucial baseline data, management of these important deep-sea environments and evidence-based decisions regarding mining will be impossible.

CRediT authorship contribution statement

Marina F. McCowin: Methodology, Software, Formal analysis, Investigation, Data curation, Writing – original draft, Writing – review & editing, Visualization. **Patrick C. Collins:** Investigation, Resources, Writing – review & editing, Funding acquisition. **Greg W. Rouse:** Conceptualization, Methodology, Formal analysis, Investigation, Resources, Writing – original draft, Writing – review & editing, Visualization, Supervision, Project administration, Funding acquisition.

Declaration of Competing Interest

The authors declare that they have no known competing financial interests or personal relationships that could have appeared to influence the work reported in this paper.

Acknowledgements

Many thanks to Cindy Van Dover, the Duke University Principal Investigator for the 2007 Luk Luk expedition, to Robert Vrijenhoek and Shannon Johnson at the Monterey Bay Aquarium Research Institute, and to the crews of the CSIRO Binatang 2000 Expedition, *R/V Melville*, and the ROV *Jason II*. Thanks also to Charlotte Seid for collection management at SIO-BIC and Shirley Sorokin at the South Australian Museum (SAM) for curation and loan of samples. We would like to thank Jonathan Mesulam and the Alliance of Solwara Warriors for their assistance in choosing a name for the newly described *Alaysia* species. Thanks also to the TAWNI program of the Chemosynthetic Ecosystems Project (ChEss) of the Census of Marine Life for support to Patrick Collins.

Funding

This work was supported by the US National Science Foundation (NSF-OCE 0939557) and the TAWNI program of the Chemosynthetic Ecosystems Project (ChEss) of the Census of Marine Life.

Appendix A. Supplementary material

Supplementary data to this article can be found online at https://doi.org/10.1016/j.ympev.2023.107872.

References

Allio, R., Schomaker-Bastos, A., Romiguier, J., Prosdocimi, F., Nabholz, B., Delsuc, F., 2020. MitoFinder: Efficient automated large-scale extraction of mitogenomic data in target enrichment phylogenomics. Mol. Ecol. Resour. 20, 892–905. https://doi.org/10.1111/1755-0998.13160.

Andersen, A.C., Hourdez, S., Marie, B., Jollivet, D., Lallier, F.H., Sibuet, M., 2004. *Escarpia southwardae* sp. nov., a new species of vestimentiferan tubeworm (Annelida, Siboglinidae) from West African cold seeps. Can. J. Zool. 82 (6), 980–999.

Bandelt, H.J., Forster, P., Rohl, A., 1999. Median-joining networks for inferring intraspecific phylogenies. Mol. Biol. Evol. 16 (1), 37–48.

Beaulieu, J.M., O'Meara, B.C., Donoghue, M.J., 2013. Identifying hidden rate changes in the evolution of a binary morphological character: The evolution of plant habit in campanulid angiosperms. Syst. Biol. 62, 725–737. https://doi.org/10.1093/sysbio/syt034.

Bernt, M., Donath, A., Jühling, F., Externbrink, F., Florentz, C., Fritzsch, G., Pütz, J., Middendorf, M., Stadler, P.F., 2013. MITOS: improved de novo metazoan mitochondrial genome annotation. Mol. Phylogenet. Evol. 69, 313–319. https://doi.org/10.1016/j.ympev.2012.08.023.

Bolger, A.M., Lohse, M., Usadel, B., 2014. Trimmomatic: a flexible trimmer for Illumina sequence data. Bioinformatics 30 (15), 2114–2120. https://doi.org/10.1093/bioinformatics/btu170.

Boore, J.L., 1999. Animal mitochondrial genomes. Nucleic Acids Res. 27, 1767–1780. https://doi.org/10.1093/nar/27.8.1767.

Bouckaert, R., Vaughan, T.G., Barido-Sottani, J., Duchêne, S., Fourment, M., Gavryushkina, A., et al., 2019. BEAST 2.5: an advanced software platform for Bayesian evolutionary analysis. PLoS Comput. Biol. 15 (4), e1006650.

Bright, M., Lallier, F., 2010. The biology of vestimentiferan tubeworms. Oceanogr. Mar. Biol. An Annu. Rev. 48, 213–265. https://doi.org/10.1201/EBK1439821169-c4.

Caullery, M., 1914. Sur les Siboglinidae, type nouveau d'invertébrés receuillis par l'expédition du Siboga. C. R. Hebd. Seances Acad. Sci. 158, 2014–2017.

Chernomor, O., Von Haeseler, A., Minh, B.Q., 2016. Terrace aware data structure for phylogenomic inference from supermatrices. Syst. Biol. 65, 997–1008. https://doi.org/10.1093/sysbio/syw037.

Collins, P.C., Kennedy, R., Van Dover, C.L., 2012. A biological survey method applied to seafloor massive sulphides (SMS) with contagiously distributed hydrothermal-vent fauna. Mar. Ecol. Prog. Ser. 452, 89–107. https://doi.org/10.3354/meps09646.

Cowart, D.A., Huang, C., Arnaud-Haond, S., Carney, S.L., Fisher, C.R., Schaeffer, S.W., 2013. Restriction to large-scale gene flow vs. regional panmixia among cold seep *Escarpia* spp. (Polychaeta, Siboglinidae). Mol. Ecol. 22, 4147–4162. https://doi.org/10.1111/mec.12379.

Darriba, D., Taboada, G.L., Doallo, R., Posada, D., 2012. jModelTest 2: more models, new heuristics and parallel computing. Nat. Methods 9, 772. https://doi.org/10.1038/nmeth.2109.

Edler, D., Klein, J., Antonelli, A., Silvestro, D., Matschiner, M., 2020. raxmlGUI 2.0: a graphical interface and toolkit for phylogenetic analyses using RAxML. Methods Ecol. Evol. 12 (2), 373–377. https://doi.org/10.1111/2041-210X.13512.

Elzanowski, A., Ostell, J., 2019. The Genetic Codes [WWW Document]. NCBI.

Feldman, R.A., Shank, T.M., Black, M.B., Baco, A.R., Smith, C.R., Vrijenhoek, R.C., 1998. Vestimentiferan on a Whale Fall. Biol. Bull. 194 (2), 116–119.

Georgieva, M.N., Little, C.T.S., Watson, J.S., Sephton, M.A., Ball, A.D., Glover, A.G., 2019. Identification of fossil worm tubes from Phanerozoic hydrothermal vents and cold seeps. J. Systematic Palaeontol. 17, 287–329. https://doi.org/10.1080/14772019.2017.1412362.

Giribet, G., Carranza, S., Baguna, J., Riutort, M., Ribera, C., 1996. First molecular evidence for the existence of a Tardigrada plus Arthropoda clade. Mol. Biol. Evol. 13, 76–84. https://doi.org/10.1093/oxfordjournals.molbev.a025573.

Halanych, K.M., 2005. Molecular phylogeny of siboglinid annelids (a.k.a. pogonophorans): a review. Hydrobiologia 535, 297–307. https://doi.org/10.1007/s10750-004-1437-6.

Halanych, K.M., Feldman, R.A., Vrijenhoek, R.C., 2001. Molecular evidence that *Sclerolinum brattstromi* is closely Related to vestimentiferans, not to frenulate pogonophorans (Siboglinidae, Annelida). Biol. Bull. 201, 65–75. https://doi.org/10.2307/1543527.

Hilário, A., Capa, M., Dahlgren, T.G., Halanych, K.M., Little, C.T.S., Thornhill, D.J., Verna, C., Glover, A.G., Laudet, V., 2011. New perspectives on the ecology and evolution of siboglinid tubeworms. PLoS One 6 (2), e16309.

Huelsenbeck, J.P., Ronquist, F., 2001. MrBayes: bayesian inference of phylogeny. Bioinformatics 17, 754–755. https://doi.org/10.1093/bioinformatics/17.8.754.

Jones, M.L., 1981. *Riftia pachyptila*, new genus, new species, the vestimentiferan worm from the Galápagos Rift geothermal vents. Biol. Soc. Washingt. 93, 1295–1313.

Jones, M.L., 1985. On the Vestimentifera, new phylum: six new species, and other taxa, from hydrothermal vents and elsewhere. Bull. Biol. Soc. Washingt. 117–158.

Jones, M.L., 1988. The Vestimentifera, their biology, systematic and evolutionary patterns. Oceanologica Acta. 69–82.

Jun, J., Won, Y.-J., Vrijenhoek, R.C., 2016. Complete mitochondrial genome of the hydrothermal vent tubeworm, *Ridgeia piscesae* (Polychaeta, Siboglinidae). Mitochondrial DNA 27, 1123–1124. https://doi.org/10.3109/19401736.2014.933330.

Katoh, K., Rozewicki, J., Yamada, K.D., 2019. MAFFT online service: multiple sequence alignment, interactive sequence choice and visualization. Brief. Bioinform. 20, 1160–1166. https://doi.org/10.1093/bib/bbx108.

Kojima, S., Ohta, S., Yamamoto, T., Miura, T., Fujiwara, Y., Fujikura, K., Hashimoto, J., 2002. Molecular taxonomy of vestimentiferans of the western Pacific and their phylogenetic relationship to species of the eastern Pacific II. Families Escarpiidae and Arcovestiidae. Mar. Biol. 141, 57–64. https://doi.org/10.1007/s00227-002-0818-5.

Kojima, S., Ohta, S., Yamamoto, T., Ymaguchi, T., Miura, T., Fujiwara, Y., Fujikura, J., Hashimoto, J., 2003. Molecular taxonomy of vestimentiferans of the western Pacific and their phylogenetic relationship to species of the eastern Pacific III. *Alaysia*-like vestimentiferans and relationships among families. Mar. Biol. 142, 625–635. https://doi.org/10.1007/s002270100581.

Kojima, S., Watanabe, H., Tsuchida, S., Fujikura, K., Rowden, A., Takai, K., Miura, T., 2006. Phylogenetic relationships of a tube worm (*Lamellibrachia juni*) from three hydrothermal vent fields in the South Pacific. J. Mar. Biol. Assoc. UK 86, 1357–1361. https://doi.org/10.1017/S002531540601438X.

Kozlov, A.M., Darriba, D., Flouri, T., Morel, B., Stamatakis, A., Wren, J., 2019. RAxML-NG: a fast, scalable and user-friendly tool for maximum likelihood phylogenetic inference. Bioinformatics 35 (21), 4453–4455.

Leigh, J., Bryant, D., 2015. PopART: full-feature software for haplotype network construction. Methods Ecol. Evol. 6, 1110–1116.

Levin, L.A., Mengerink, K., Gjerde, K.M., Rowden, A.A., Van Dover, C.L., Clark, M.R., Ramirez-Llodra, E., Currie, B., Smith, C.R., Sato, K.N., Gallo, N., Sweetman, A.K., Lily, H., Armstrong, C.W., Brider, J., 2016. Defining "serious harm" to the marine environment in the context of deep-seabed mining. Mar. Policy 74, 245–259. https://doi.org/10.1016/j.marpol.2016.09.032.

Li, Y., Kocot, K.M., Schander, C., Santos, S.R., Thornhill, D.J., Halanych, K.M., 2015. Mitogenomics reveals phylogeny and repeated motifs in control regions of the deep-sea family Siboglinidae (Annelida). Mol. Phylogenet. Evol. 85, 221–229. https://doi.org/10.1016/j.ympev.2015.02.008.

Li, Y., Kocot, K.M., Whelan, N.V., Santos, S.R., Waits, D.S., Thornhill, D.J., Halanych, K.M., 2017. Phylogenomics of tubeworms (Siboglinidae, Annelida) and comparative performance of different reconstruction methods. Zool. Scr. 46, 200–213. https://doi.org/10.1111/zsc.12201.

Li, Leilei, Wang, M., Li, Lifeng, Du, Z., Sun, Y., Wang, X., Zhang, X., Li, C., 2020. Endosymbionts of Metazoans Dwelling in the PACManus Hydrothermal Vent: Diversity and Potential Adaptive Features Revealed by Genome Analysis. Appl. Environ. Microbiol. 86, 1–22. https://doi.org/10.1128/AEM.00815-20.

Little, C.T.S., Cann, J.R., Herrington, R.J., Morisseau, M., 1999. Late Cretaceous hydrothermal vent communities from the Troodos ophiolite, Cyprus. Geology 27, 1027–1030. https://doi.org/10.1130/0091-7613(1999)027<1027:LCHVCF>2.3.CO;2.

Little, C.T.S., Danelian, T., Herrington, R.J., Haymon, R.M., 2004. Early Jurassic hydrothermal vent community from the Franciscan complex, California. Geology 27, 167–170. https://doi.org/10.1666/0022-3360(2004)078<0542:EJHVCF>2.0.CO;2.

Little, C., Vrijenhoek, R.C., 2003. Are hydrothermal vent animals living fossils? Trends in Ecol Evolution 18, 582–588. https://doi.org/10.1016/j.tree.2003.08.009.

Maddison, W.P., Maddison, D.R., 2018. Mesquite: a modular system for evolutionary analysis. Version 3.51.

McCowin, M.F., Rouse, G.W., 2018. A new *Lamellibrachia* species and confirmed range extension for *Lamellibrachia barhami* (Siboglinidae, Annelida) from Costa Rica methane seeps. Zootaxa 4504, 1–22. https://doi.org/10.11646/zootaxa.4504.1.1.

McCowin, M.F., Rowden, A.A., Rouse, G.W., 2019. A new record of *Lamellibrachia columna* (Siboglinidae, Annelida) from cold seeps off New Zealand, and an assessment of its presence in the western Pacific Ocean. Mar. Biodivers. Rec. 12, 12. https://doi.org/10.1186/s41200-019-0169-2.

Miglietta, M.P., Hourdez, S., Cowart, D.A., Schaeffer, S.W., Fisher, C., 2010. Species boundaries of Gulf of Mexico vestimentiferans (Polychaeta, Siboglinidae) inferred

from mitochondrial genes. Deep. Res. Part II Top. Stud. Oceanogr. 57, 1916–1925. https://doi.org/10.1016/j.dsr2.2010.05.007.
Miller, K.A., Thompson, K.F., Johnston, P., Santillo, D., 2018. An overview of seabed mining Including the current state of development, environmental impacts, and knowledge gaps. Front. Mar. Sci. 4 https://doi.org/10.3389/fmars.2017.00418.
Miura, T., Kojima, S., 2006. Two new species of vestimentiferan tubeworm (Polychaeta: Siboglinidae a.k.a. Pogonophora) from the Brothers Caldera, Kermadec ArcTwo New Species of Vestimentiferan Tubeworm (Polychaeta: Siboglinidae a.k.a. Pogonophora) from the Brothers Caldera, Kermadec Arc, South Pacific Ocean. South Pacific Ocean. Species Divers. 11 (3), 209–224.
Nagarajan, N., Pop, M., 2013. Sequence assembly demystified. Nat. Rev. Genet. 14, 157–167. https://doi.org/10.1038/nrg3367.
Nelson, K., Fisher, C.R., 2000. Absence of cospeciation in deep-sea vestimentiferan tube worms and their bacterial endosymbionts. Symbiosis 28, 1–15. https://doi.org/10.2307/25066661.
Palumbi, S.R., 1996. Nucleic acid II: the polymerase chain reaction, in: Hillis, D.M., Moritz, C., Mable, B.K. (Eds.), Molecular Systematics. Sinauer Associates, Inc, Sunderland, MA, pp. 205–247.
Pante, E., Simon-Bouhet, B., 2013. marmap: a package for importing, plotting and analyzing bathymetric and topographic data in R. PLoS One 8 (9), e73051.
Patra, A.K., Kwon, Y.M., Kang, S.G., Fujiwara, Y., Kim, S.J., 2016. The complete mitochondrial genome sequence of the tubeworm *Lamellibrachia satsuma* and structural conservation in the mitochondrial genome control regions of Order Sabellida. Mar. Genomics 26, 63–71. https://doi.org/10.1016/j.margen.2015.12.010.
Pleijel, F., Dahlgren, T.G., Rouse, G.W., 2009. Progress in systematics: from siboglinidae to pogonophora and vestimentifera and back to siboglinidae. C. R. Biol. 332, 140–148. https://doi.org/10.1016/J.CRVI.2008.10.007.
Plouviez, S., Jacobson, A., Wu, M., Van Dover, C.L., 2014. Characterization of vent fauna at the mid-Cayman spreading center. Deep. Res. Part I Oceanogr. Res. Pap. 97, 124–133. https://doi.org/10.1016/j.dsr.2014.11.011.
Rambaut, A., Drummond, A.J., Xie, D., Baele, G., Suchard, M.A., Susko, E., 2018. Posterior summarization in Bayesian phylogenetics using Tracer 1.7. Syst. Biol. 67 (5), 901–904. https://doi.org/10.1093/sysbio/syy032.
Revell, L.J., 2012. phytools: an R package for phylogenetic comparative biology (and other things). Methods Ecol. Evol. 3, 217–223.
Ronquist, F., Huelsenbeck, J.P., 2003. MRBAYES 3: Bayesian phylogenetic inference under mixed models. Bioinformatics 19, 1572–1574.
Rouse, G.W., Fauchald, K., 1997. Cladistics and polychaetes. Cladistics and polychaetes. Zool. Scr. 26 (2), 139–204. https://doi.org/10.1111/j.1463-6409.1997.tb00412.x.
Pradillon, F., Kawato, M., Fujikura, K., Noda, C., Fujiwara, Y., 2009. Diversity, colonization and succession patterns of *Osedax* species from a sperm-whale carcass in Sagami Bay, Japan. Extremobiosphere Research Center, Japan Agency for Marine-Earth. Science and Technology 2-15.
Samadi, S., Puillandre, N., Pante, E., Boisselier, M.C., Corbari, L., Chen, W.J., Maestrati, P., Mana, R., Thubaut, J., Zuccon, D., Hourdez, S., 2015. Patchiness of deep-sea communities in Papua New Guinea and potential susceptibility to anthropogenic disturbances illustrated by seep organisms. Mar. Ecol. 36, 109–132. https://doi.org/10.1111/maec.12204.
Shen, W., Le, S., Li, Y., Hu, F., Zou, Q., 2016. SeqKit: a cross-platform and ultrafast Toolkit for FASTA/Q File manipulation. PLoS One 11 (10), e0163962.
Shimodaira, H., 2002. An approximately unbiased test of phylogenetic tree selection. Syst. Biol. 51 (3), 492–508. https://doi.org/10.1080/10635150290069913.
Southward, E.C., 1991. Three new species of Pogonophora, including two vestimentiferans, from hydrothermal sites in the lau back-arc basin (Southwest pacific ocean). J. Nat. Hist. 25, 859–881. https://doi.org/10.1080/00222939100770571.
Southward, E.C., Andersen, A.C., Hourdez, S., 2011. *Lamellibrachia anaximandri* n. sp., a new vestimentiferan tubeworm (Annelida) from the Mediterranean, with notes on frenulate tubeworms from the same habitat. Zoosystema 33, 245–279. https://doi.org/10.5252/z2011n3a1.
Southward, E.C., Galkin, S.V., 1997. A new vestimentiferan (Pogonophora: Obturata) from hydrothermal vent fields in the Manus Back-arc Basin (Bismarck Sea, Papua New Guinea, Southwest Pacific Ocean). J. Nat. Hist. 31, 43–55. https://doi.org/10.1080/00222939700770041.
Southward, E.C., Schulze, A., Tunnicliffe, V., 2002. Vestimentiferans (Pogonophora) in the Pacific and Indian Oceans: a new genus from Lihir Island (Papua New Guinea) and the Java Trench, with the first report of *Arcovestia ivanovi* from the North Fiji Basin. J. Nat. Hist. 36, 1179–1197. https://doi.org/10.1080/00222930110040402.
Stiller, J., Rousset, V., Pleijel, F., Chevaldonné, P., Vrijenhoek, R.C., Rouse, G.W., 2013. Phylogeny, biogeography and systematics of hydrothermal vent and methane seep *Amphisamytha* (Ampharetidae, Annelida), with descriptions of three new species. Systematics and Biodiversity 11, 35–65. https://doi.org/10.1080/14772000.2013.772925.
Sun, Y., Liang, Q., Sun, J., Yang, Y., Tao, J., Liang, J., Feng, D., Qiu, J.-W., Qian, P.-Y., 2018. The mitochondrial genome of the deep-sea tubeworm *Paraescarpia echinospica* (Siboglinidae, Annelida) and its phylogenetic implications. Mitochondrial DNA Part B 3, 131–132. https://doi.org/10.1080/23802359.2018.1424576.
Swofford, D.L., 2003. PAUP *. Phylogenetic Analysis Using Parsimony (* and Other Methods); Version 4.
Taboada, S., Riesgo, A., Bas, M., Arnedo, M.A., Cristobo, J., Rouse, G.W., Avila, C., Kiel, S., 2015. Bone-eating worms spread: Insights into shallow-water *Osedax* (Annelida, Siboglinidae) from Antarctic, Subantarctic, and Mediterranean waters. PLoS ONE 10 (11), e0140341.
Trevisan, B., Alcantara, D.M.C., Machado, D.J., Marques, F.P.L., Lahr, D.J.G., 2019. Genome skimming is a low-cost and robust strategy to assemble complete mitochondrial genomes from ethanol preserved specimens in biodiversity studies. PeerJ 7, e7543.
Van Audenhaege, L., Fariñas-Bermejo, A., Schultz, T., Lee Van Dover, C., 2019. An environmental baseline for food webs at deep-sea hydrothermal vents in Manus Basin (Papua New Guinea). Deep. Res. Part I Oceanogr. Res. Pap. 148, 88–99. https://doi.org/10.1016/j.dsr.2019.04.018.
Vrijenhoek, R.C., 2013. On the instability and evolutionary age of deep-sea chemosynthetic communities. Deep-Sea Res Pt II 92, 189–200. https://doi.org/10.1016/j.dsr2.2012.12.004.
Watanabe, H., Kojima, S., 2015. Subseafloor Biosphere Linked to Hydrothermal Systems: TAIGA Concept, in: Ishibashi, J., Okino, K., Sunamura, M. (Eds.), Subseafloor Biosphere Linked to Hydrothermal Systems: TAIGA Concept. Springer Japan, Tokyo, pp. 449–459. 10.1007/978-4-431-54865-2.
Webb, M., 1964. A new bitentaculate pogonophoran from Hardangerfjorden, Norway. Sarsia 15, 9–55.
Webb, M., 1969. *Lamellibrachia barhami*, gen. nov., sp. nov. (Pogonophora), from the Northeast Pacific. Bull. Mar. Sci. 19, 18–47.
Whiting, M.F., Carpenter, J.C., Wheeler, Q.D., Wheeler, W.C., 1997. The *stresiptera* problem: phylogeny of the holometabolous insect orders inferred from 18S and 28S Ribosomal DNA Sequences and Morphology. Syst. Biol. 46, 1. https://doi.org/10.2307/2413635.
Xia, X., 2013. DAMBE5: a comprehensive software package for data analysis in molecular biology and evolution. Mol. Biol. Evol. 30, 1720–1728. https://doi.org/10.1093/molbev/mst064.
Xia, X., Lemey, P., 2012. Assessing substitution saturation with DAMBE. Phylogenetic Handb. 615–630 https://doi.org/10.1017/cbo9780511819049.022.
Xia, X., Xie, Z., Salemi, M., Chen, L., Wang, Y., 2003. An index of substitution saturation and its application. Mol. Phylogenet. Evol. 26, 1–7. https://doi.org/10.1016/S1055-7903(02)00326-3.